Supporting Information

Influence of Heteroatoms on Circularly Polarized Luminescence Performance for [7]Helicene Derivatives：Non-aromatic vs. Aromatic Five-membered Rings

Yan Liu,[a] Zhiying Ma,*[a] Hang Su,[a] Ran Wei,[a] Zhitao Shen*[b,c] and Hua Wang[a]

[a] *Engineering Research Center for Nanomaterials, Henan University, Kaifeng, 475004, China*

[b] *School of Future Technology, Henan University, Kaifeng 475004, China*

[c] *Institute of Quantum Materials and Physics, Henan Academy of Sciences, Zhengzhou 450046, China*

* *Correspondence: mazy11@henu.edu.cn, shenzt@vip.henu.edu.cn*

Contents

I. Supplementary benchmarks

It is well known that B3LYP, PBE0[1], M06-2X[2], ωB97XD[3] and CAM-B3LYP[4] are suitable exchange-correlation functionals for calculating excited states geometries of the aromatic compounds.[5] Combined with the fact that B3LYP are well-recognized and widely used for ground state structure calculation. Thus, on the basis of the optimized ground state structure using B3LYP, we selected the above five different functionals in conjunction with 6-311G (2d, p) basis set to optimize the S_1 state of **[7]H** and **[7]H-C**. As shown in the Table S2, the calculated emission energies of **[7]H** and **[7]H-C** both decrease with the increasing of HF exchange component, and the mean average error of the B3LYP is the smallest. On the other hand, this method reproduces both the photophysical and transition parameters at the expense of the computation of the emission energy, which appears to be the most suitable TDDFT method to estimate the excited state properties for the helicene systems.

To survey the dependance of g_{lum} on the functionals, the data of transition properites of **[7]H-C** are collectively given in the Table S5. Calculations show that the absolute values of each axis component of transition electronic dipole moment (**μ**) and transition magnetic dipole moment (**m**), the angles between μ and m, and the g_{lum} are slightly affected by the different functionals. In addition, the effect of basis sets on g_{lum} have also been considered. Table S6 collects the quantities **μ**, **m**, and the g_{lum} based on the optimized geometry by B3LYP in conjunction with two minimum acceptable size (6-31G(d) and 6-311G(d)), two medium-sized (6-311G(2d, p), def-TZVP), and more expensive (def2-TZVP[6]) basis sets. The data show that as the basis sets increases, the g_{lum} first increases and then levels off implying that the inexpensive B3LYP/6-311G(2d, p) level is adequate for exploring transition properties of the [7]helicene derivative and analogous compounds. Therefore, the B3LYP exchange-correlation functional in combination with the 6-311G(2d, p) basis set was used in our study.

References

1. Adamo and V. Barone, *J. Chem.Phys.*, 1999, **110**, 6158-6170.
2. Y. Zhao and D. G. Truhlar, *Theor. Chem. Acc.*, 2008, **120**, 215-241.
3. J.-D. Chai and M. Head-Gordon, *Phys.Chem. Chem. Phys.*, 2008, **10**, 6615-6620.
4. T. Yanai, D. P. Tew and N. C. Handy, *Chem. Phys. Lett.*, 2004, **393**, 51-57.
5. J. Wang and B. Durbeej, *J. Comput. Chem*., 2020, **41**, 1718-1729.
6. F. Weigend and R. Ahlrichs, *Phys. Chem. Chem. Phys.*, 2005, **7**, 3297-3305.

II. Supplementary Tables S1-S6

Table S1. Selected bond lengths and dihedral angles variations between S_0 and S_1 states for [7]helicene derivatives.

[7]H			**[7]H-C**	**[7]H-Si**	**[7]H-Ge**		**[7]H-O**	**[7]H-S**	**[7]H-Se**
C1-C2	0.021	C3-C4	0.029	0.037	0.035	C3-C4	0.025	0.023	0.024
C3-C4	0.029	C4-C5	-0.068	-0.079	-0.076	C4-C5	-0.048	-0.065	-0.065
C5-C6	0.029	C5-C6	0.029	0.037	0.035	C5-C6	0.025	0.023	0.024
C7-C8	0.023	C7-C11	-0.031	-0.034	-0.035	C7-C11	-0.024	-0.033	-0.034
C21-C22	0.023	C9-C10	0.034	0.032	0.034	C9-C10	0.032	0.041	0.041
		C19-C20	0.034	0.032	0.034	C19-C20	0.032	0.041	0.041
		C22-C26	-0.031	-0.034	-0.035	C22-C26	-0.024	-0.033	-0.034
		C3-C19		-0.021	-0.022	C3-C19		-0.023	-0.023
		C4-C22		0.029	0.031	C6-C10		-0.023	-0.023
		C5-C7		0.029	0.031	C4-C22			0.020
		C6-C10		-0.021	-0.022	C5-C7			0.020
						C3-X			0.021
						C6-X			0.021
		C4-C5-C6-C10	0.15	-0.19	-0.19	C4-C5-C6-C10		0.15	0.16
		C4-C5-C7-C8	-0.19	0.20	0.19	C4-C5-C7-C8		-0.20	-0.19
		C4-C5-C7-C11	-0.19	0.23	0.23	C4-C5-C7-C11		-0.22	-0.22
		C5-C4-C3-C19	0.15	-0.19	-0.19	C5-C4-C22-C21		-0.20	-0.19
		C5-C4-C22-C21	-0.19	0.20	0.19	C5-C4-C22-C26		-0.22	-0.22
		C5-C4-C22-C26	-0.19	0.23	0.23	C7-C5-C4-C22		0.17	0.19
		C7-C5-C4-C22	0.15	-0.25	-0.26	C19-C3-C4-C5		0.15	0.16
		C3-C4-C5-C7		-0.15	-0.16				
		C6-C5-C4-C22		-0.15	-0.16				
		H-C-C3-C19		0.29	0.29				
		H-C-C6-C10		0.29	0.29				

Table S2. Calculated emission energies (ΔE_{cal}), the experimental values (ΔE_{exp}), the deviation between calculation and experimental for **[7]H** and **[7]H-C** optimized at different density functional levels.

		[7]H			**[7]H-C**			
Method	HF%[a]	ΔE_{cal}	ΔE_{exp}	$\lvert \Delta E_{cal-exp} \rvert$	ΔE_{cal}	ΔE_{exp}	$\lvert \Delta E_{cal-exp} \rvert$	MAE[b]
B3LYP	20%	447	476	29	465	417	48	39
PBE0	25%	431		45	453		36	41
M062X	54%	398		78	429		12	45
CAM-B3LYP	19~65%	392		84	430		13	48
ωB97XD	22.2~100%	391		85	426		9	47

[a] Hartree-Fock exchange component. For range-separated functionals CAM-B3LYP and ωB97XD, the values refer to the compositions of the short and long ranges of interelectronic interaction.

[b] MAE refers to mean average error.

Table S3. Relaxation energies of low-frequency modes (λ_l) and high-frequency modes (λ_h) as well as the total reorganization energy (λ) of [7]helicene and its derivations in solution phase.

Compounds	λ_l	λ_h	λ
[7]H	84	189	284
[7]H-C	292	275	610
[7]H-Si	470	393	900
[7]H-Ge	471	406	919
[7]H-O	145	219	383
[7]H-S	419	354	828
[7]H-Se	443	377	878

Table S4. Selected computational excitation wavelength (λ), oscillator strength (*f*) and transition nature for the helicenes.

		states	λ/eV	λ/nm	*f*	Transition Contributions
[7]H	Band I	$S_0 \rightarrow S_1$	3.04	407	0.0003	H → L (61%), H-1 → L+1 (38%)
		$S_0 \rightarrow S_2$	3.21	386	0.0197	H-1 → L (93%), H → L+1 (6%)
		$S_0 \rightarrow S_3$	3.26	380	0.0549	H → L+1 (85%), H-2 → L (9%)
	Band II	$S_0 \rightarrow S_4$	3.50	354	0.0381	H-2 → L (74%), H-1 → L+2 (12%), H-3 → L+1 (6%), H → L+1 (6%)
		$S_0 \rightarrow S_5$	3.54	350	0.0124	H-1 → L+1 (54%), H → L (33%), H-2 → L+1 (10%)
		$S_0 \rightarrow S_6$	363	342	0.0310	H-2 → L+1 (73%), H → L+2 (10%), H-3 → L (7%)
	Band III	$S_0 \rightarrow S_8$	3.93	315	0.0324	H-3 → L+1 (53%), H → L+3 (31%), H-2 → L (10%)
		$S_0 \rightarrow S_9$	3.96	313	0.0383	H-1 → L+2 (68%), H-3 → L+1 (22%)
		$S_0 \rightarrow S_{10}$	4.02	308	0.0694	H-1 → L+3 (42%), H → L+2 (32%), H-3 → L (16%), H-2 → L+1 (6%)
	Band IV	$S_0 \rightarrow S_{16}$	4.53	274	0.3640	H-1 → L+3 (37%), H-5 → L+1 (24%), H-3 → L (10%), H → L+2 (9%), H-3 → L+2 (8%)
		$S_0 \rightarrow S_{17}$	4.70	264	0.1228	H-5 → L (36%), H → L+4 (27%), H-1 → L+5 (9%)
		$S_0 \rightarrow S_{18}$	4.72	263	0.3539	H-3 → L+2 (34%), H-5 → L+1 (23%), H-2 → L+3 (11%), H-1 → L+3 (8%), H-1 → L+4 (6%)
		$S_0 \rightarrow S_{20}$	4.84	256	0.1151	H → L+4 (64%), H-1 → L+5 (11%), H-3 → L+3 (10%), H-5 → L (6%)
[7]H-C	Band I	$S_0 \rightarrow S_1$	3.20	387	0.1581	H → L (89%), H → L+1 (7%)
	Band II	$S_0 \rightarrow S_3$	3.55	350	0.0359	H → L+1 (53%), H-2 → L (37%), H → L (7%)
		$S_0 \rightarrow S_4$	3.76	330	0.0362	H-2 → L (60%), H → L+1 (36%)
		$S_0 \rightarrow S_5$	3.85	322	0.0856	H → L+2 (64%), H-1 → L (15%), H-3 → L (6%), H → L+3 (5%)
	Band III	$S_0 \rightarrow S_6$	3.98	312	0.0184	H-3 → L (56%), H-1 → L+1 (26%), H-2 → L+2 (6%), H → L+2 (5%)
		$S_0 \rightarrow S_8$	4.15	298	0.0534	H-1 → L+2 (86%), H-4 → L

						(6%)
	Band IV	$S_0 \rightarrow S_{14}$	4.60	270	0.1695	H-2 → L+2 (34%), H → L+3 (16%), H-2 → L+3 (10%), H-1 → L+1 (10%), H-5 → L (9%), H-3 → L (8%)
		$S_0 \rightarrow S_{16}$	4.80	258	0.0831	H-1 → L+3 (36%), H-3 → L+2 (32%), H-4 → L+1 (16%)
	Band V	$S_0 \rightarrow S_{18}$	5.01	248	0.0694	H → L+5 (60%), H-4 → L+2 (19%), H-2 → L+3 (6%)
		$S_0 \rightarrow S_{20}$	5.05	246	0.0391	H-4 → L+1 (53%), H-3 → L+3 (12%), H-2 → L+4 (10%), H-1 → L+3 (8%), H → L+6 (7%)
		$S_0 \rightarrow S_{21}$	5.11	242	0.1846	H-2 → L+3 (39%), H-1 → L+4 (26%), H-4 → L+2 (24%)
		$S_0 \rightarrow S_{22}$	5.20	238	0.4172	H-4 → L+2 (22%), H-5 → L+1 (19%), H-2 → L+3 (12%), H → L+5 (11%), H-5 → L (11%), H-3 → L+1 (8%)
[7]H-Si	Band I	$S_0 \rightarrow S_1$	3.11	399	0.0980	H → L (92%)
	Band II	$S_0 \rightarrow S_4$	3.49	355	0.0477	H → L+1 (55%), H-1 → L (40%)
	Band III	$S_0 \rightarrow S_5$	3.78	328	0.0188	H → L+2 (43%), H-3 → L (37%), H-2 → L (10%)
		$S_0 \rightarrow S_6$	3.82	325	0.0293	H-3 → L (48%), H → L+2 (31%), H-2 → L+1 (5%)
		$S_0 \rightarrow S_7$	3.85	322	0.0889	H-1 → L+1 (94%)
	Band IV	$S_0 \rightarrow S_{13}$	4.46	278	0.0452	H-3 → L+2 (66%), H-2 → L+3 (11%), H-2 → L+2 (8%), H-4 → L (8%)
		$S_0 \rightarrow S_{14}$	4.48	277	0.1756	H-5 → L (27%), H → L+3 (25%), H-1 → L+2 (21%), H-2 → L+1 (7%), H-3 → L (7%), H-1 → L+3 (6%)
	Band V	$S_0 \rightarrow S_{18}$	4.87	254	0.5678	H-1 → L+3 (46%), H-5 → L (10%), H-5 → L+1 (7%), H-3 → L+1 (7%), H → L+3 (7%)
		$S_0 \rightarrow S_{19}$	4.96	250	0.0787	H-2 → L+3 (52%), H-1 → L+4 (10%), H-4 → L+1 (9%), H-5 → L+2 (8%), H-3 → L+2 (5%)
		$S_0 \rightarrow S_{23}$	5.12	242	0.1302	H-4 → L+2 (33%), H → L+5 (31%), H-2 → L+4 (10%), H-5 → L (7%)
[7]H-Ge	Band I	$S_0 \rightarrow S_1$	3.11	398	0.0959	H → L (92%)
	Band II	$S_0 \rightarrow S_4$	3.55	350	0.0439	H → L+1 (68%), H-1 → L

						(25%)
	Band III	$S_0 \rightarrow S_6$	3.83	324	0.0329	H-3 → L (41%), H → L+2 (38%), H-2 → L (6%)
		$S_0 \rightarrow S_7$	3.89	319	0.0899	H-1 → L+1 (94%)
	Band IV	$S_0 \rightarrow S_{13}$	4.45	279	0.0437	H-3 → L+2 (65%), H-2 → L+3 (15%), H-2 → L+2 (8%), H-4 → L (7%)
		$S_0 \rightarrow S_{14}$	4.48	277	0.1661	H-5 → L (37%), H → L+3 (21%), H-1 → L+2 (18%), H-2 → L+1 (8%), H-3 → L (6%)
	Band V	$S_0 \rightarrow S_{18}$	4.84	256	0.5443	H-1 → L+3 (45%), H-5 → L (8%), H → L+3 (8%), H-3 → L+1 (7%), H-5 → L+1 (5%)
		$S_0 \rightarrow S_{19}$	4.95	251	0.0639	H-2 → L+3 (41%), H-4 → L+1 (14%), H-1 → L+4 (10%), H-5 → L+2 (9%), H → L+4 (7%)
		$S_0 \rightarrow S_{25}$	5.18	239	0.1535	H-6 → L (53%), H-8 → L (21%)
[7]H-O	Band I	$S_0 \rightarrow S_1$	3.33	373	0.1448	H → L (89%)
		$S_0 \rightarrow S_2$	3.35	370	0.0141	H-1 → L (81%), H → L+1 (15%)
	Band II	$S_0 \rightarrow S_4$	3.90	318	0.0946	H → L+1 (72%), H-1 → L (12%), H-3 → L (10%)
		$S_0 \rightarrow S_5$	3.94	315	0.1928	H-1 → L+1 (92%)
	Band III	$S_0 \rightarrow S_{13}$	4.63	268	0.1096	H-2 → L+1 (31%), H-2 → L+3 (19%), H → L+3 (14%), H-1 → L+2 (14%), H-3 → L (7%), H-3 → L+2 (7%)
		$S_0 \rightarrow S_{15}$	4.76	260	0.0923	H-5 → L (39%), H-3 → L+1 (15%), H-4 → L+1 (13%), H-1 → L+3 (11%), H-2 → L+2 (6%)
		$S_0 \rightarrow S_{16}$	4.80	258	0.0786	H-3 → L+2 (54%), H-2 → L+3 (11%), H → L+3 (9%), H-3 → L (7%)
	Band IV	$S_0 \rightarrow S_{22}$	5.21	238	0.4650	H-2 → L+3 (25%), H-3 → L+2 (16%), H-5 → L+1 (16%), H-4 → L+2 (14%), H → L+4 (8%)
[7]H-S	Band I	$S_0 \rightarrow S_1$	3.16	392	0.0233	H-1 → L (89%), H → L+1 (8%)
		$S_0 \rightarrow S_2$	3.19	389	0.1015	H → L (91%)
	Band II	$S_0 \rightarrow S_4$	3.79	327	0.1223	H-1 → L+1 (93%)
		$S_0 \rightarrow S_5$	3.84	323	0.0421	H → L+1 (78%), H-3 → L (10%), H-1 → L (5%)
		$S_0 \rightarrow S_8$	4.03	308	0.0877	H-1 → L+2 (35%), H-3 → L (24%), H-2 → L+1 (17%), H → L+3 (10%), H → L+1 (7%)

	Band III	$S_0 \rightarrow S_{13}$	4.48	277	0.1259	H-2 → L+1 (20%), H-3 → L+2 (19%), H-2 → L+3 (19%), H → L+3 (18%), H-1 → L+4 (7%), H-1 → L+2 (6%), H-5 → L+1 (5%)
		$S_0 \rightarrow S_{15}$	4.62	269	0.0962	H-3 → L+1 (32%), H-4 → L+1 (24%), H-1 → L+3 (21%), H-5 → L (11%)
		$S_0 \rightarrow S_{16}$	4.64	267	0.1057	H-3 → L+2 (50%), H → L+3 (21%), H-2 → L+3 (7%)
	Band IV	$S_0 \rightarrow S_{19}$	4.92	252	0.0868	H-4 → L+1 (61%), H-3 → L+1 (7%), H-2 → L+4 (6%)
		$S_0 \rightarrow S_{20}$	4.97	249	0.1561	H-4 → L+2 (53%), H → L+5 (16%), H-2 → L+3 (8%), H-1 → L+4 (7%)
		$S_0 \rightarrow S_{21}$	5.04	246	0.1609	H-1 → L+6 (35%), H-2 → L+3 (24%), H-5 → L+1 (17%), H-1 → L+7 (7%)
		$S_0 \rightarrow S_{23}$	5.07	245	0.3470	H-5 → L+1 (22%), H-3 → L+2 (12%), H-4 → L+2 (12%), H → L+5 (8%), H-2 → L+3 (8%), H-1 → L+4 (8%), H-1 → L+6 (7%), H-5 → L+3 (5%)
[7]H-Se	Band I	$S_0 \rightarrow S_1$	3.06	405	0.0271	H → L (92%)
		$S_0 \rightarrow S_2$	3.13	396	0.1020	H-1 → L (93%)
	Band II	$S_0 \rightarrow S_4$	3.75	331	0.0794	H → L+1 (93%)
		$S_0 \rightarrow S_8$	3.94	315	0.0921	H → L+2 (42%), H-3 → L (20%), H-2 → L+1 (17%), H-1 → L+1 (8%), H-1 → L+3 (6%)
	Band III	$S_0 \rightarrow S_{16}$	4.47	277	0.0857	H-3 → L+2 (33%), H-2 → L+3 (32%), H-2 → L+1 (10%), H-1 → L+3 (6%), H → L+4 (6%)
		$S_0 \rightarrow S_{17}$	4.59	270	0.1854	H-1 → L+3 (35%), H-3 → L+2 (34%), H-2 → L+1 (7%), H → L+2 (6%), H-3 → L (5%)
		$S_0 \rightarrow S_{18}$	4.59	270	0.0944	H-3 → L+1 (42%), H-4 → L+1 (21%), H → L+3 (18%)
		$S_0 \rightarrow S_{19}$	4.84	256	0.0639	H-4 → L+1 (61%), H-2 → L+4 (15%), H-3 → L+1 (6%)
		$S_0 \rightarrow S_{20}$	4.85	256	0.1974	H-4 → L+2 (52%), H-2 → L+3 (25%), H-3 → L+2 (7%)
		$S_0 \rightarrow S_{21}$	4.93	251	0.2052	H-4 → L+2 (29%), H-2 → L+3 (28%), H → L+5 (13%), H-3 → L+2 (10%), H-6 → L (6%)
		$S_0 \rightarrow S_{29}$	5.26	236	0.2799	H-6 → L (61%), H-5 → L+1

						(9%), H-1 → L+6 (6%)

Table S5. Transition properties of **[7]H-C** optimized using different density functionals in conjunction with 6-311G(2d, p) basis set.

	B3LYP	PBE0	M06-2X	CAM-B3LYP	ωB97XD
HF exchange	20%	25%	54%	19~65%	22.2~100%
μ and **m** in atom units [a]					
μ_x	-1.5610	-1.5720	-1.6226	-1.6507	-1.6454
μ_y	-0.0001	-0.0003	0.0000	0.0000	0.0001
μ_z	-0.3864	-0.3833	0.3652	-0.3514	-0.3447
$\lvert\boldsymbol{\mu}\rvert$	1.6081	1.6181	1.6632	1.6877	1.6811
m_x	-0.1022	-0.1305	-0.1356	-0.1568	-0.1362
m_y	0.0000	0.0000	0.0000	0.0000	0.0000
m_z	-1.9410	-2.0108	2.1513	-2.0302	-2.0352
$\lvert\boldsymbol{m}\rvert$	1.9437	2.0150	2.1556	2.0362	2.0398
Transition parameters in CGS units					
μ_x [b]	-396.7594	-399.5552	-412.4162	-419.5584	-418.2113
μ_y [b]	-0.0254	-0.0763	0.0000	0.0000	0.0254
μ_z [b]	-98.2113	-97.4234	92.8229	-89.3153	-87.6124
$\lvert\boldsymbol{\mu}\rvert$ [b]	408.7340	411.2611	422.7331	428.9598	427.2899
m_x [b]	0.3583	0.3555	-0.3387	0.3259	0.3197
m_y [b]	-1.4914	-1.5006	-1.5425	-1.5652	-1.5591
m_z [b]	367.9551	370.5479	382.4752	389.0989	387.8496
$\lvert\boldsymbol{m}\rvert$ [b]	1.8026	1.8687	1.9991	1.8884	1.8917
$\lvert\boldsymbol{\mu}\rvert/\lvert\boldsymbol{m}\rvert$	226.7496	220.0739	211.4641	227.1531	225.8799
θ [c]	106.9	107.4	106.3	106.4	105.7
$\cos\theta$	-0.2910	-0.2993	-0.2805	-0.2829	-0.2699
g_{lum}	-0.0051	-0.0054	-0.0053	-0.0050	-0.0048

[a] Transition electric dipole moment **μ** and transition magnetic dipole moment **m** are in a.u.

[b] **μ** and **m** are in 10^{-20} esu·cm and 10^{-20} erg·G^{-1}, respectively.

[c] θ (in deg) represents the angle between **μ** and **m**.

Table S6. Transition properties of **[7]H-C** optimized via B3LYP exchange-correlation functional in conjunction with different basis sets

	6-31G(d)	6-311G(d)	6-311G(2d,p)	def-TZVP	def2-TZVP
μ and **m** in atom units [a]					
μ_x	-1.6265	-1.5832	-1.5610	-1.5598	-1.5544
μ_y	0.0000	-0.0003	-0.0001	0.0009	0.0003
μ_z	-0.3898	-0.3920	-0.3864	0.3663	0.3636
$\lvert\boldsymbol{\mu}\rvert$	1.6726	1.6310	1.6081	1.6022	1.5964
m_x	-0.0618	-0.0805	-0.1022	-0.1172	-0.1170
m_y	0.0000	0.0000	0.0000	-0.0001	0.0000
m_z	-1.7896	-1.8981	-1.9410	1.9439	1.9667
$\lvert\boldsymbol{m}\rvert$	1.7907	1.8998	1.9437	1.9474	1.9702
Transition parameters in CGS units					
μ_x [b]	-413.4075	-402.4019	-396.7594	-396.4544	-395.0818
μ_y [b]	0.0000	-0.0763	-0.0254	0.2288	0.0763
μ_z [b]	-99.0755	-99.6346	-98.2113	93.1025	92.4162
$\lvert\boldsymbol{\mu}\rvert$ [b]	425.1138	414.5532	408.7340	407.2397	405.7468
m_x [b]	0.0573	0.0747	0.0948	0.1087	0.1085
m_y [b]	0.0000	0.0000	0.0000	0.0001	0.0000
m_z [b]	1.6597	1.7603	1.8001	-1.8028	-1.8239
$\lvert\boldsymbol{m}\rvert$ [b]	1.6607	1.7619	1.8026	1.8060	1.8271
$\lvert\boldsymbol{\mu}\rvert/\lvert\boldsymbol{m}\rvert$	255.9899	235.2900	226.7496	225.4866	222.0661
θ [c]	105.5	106.3	106.9	106.7	106.6
$\cos\theta$	-0.2665	-0.2813	-0.2910	-0.2868	-0.2852
g_{lum}	-0.0042	-0.0048	-0.0051	-0.0051	-0.0051

[a] Transition electric dipole moment **μ** and transition magnetic dipole moment **m** are in a.u.

[b] **μ** and **m** are in 10^{-20} esu·cm and 10^{-20} erg·G^{-1}, respectively.

[c] θ (in deg) represents the angle between **μ** and **m**.

III. Supplementary Figures S1-S12

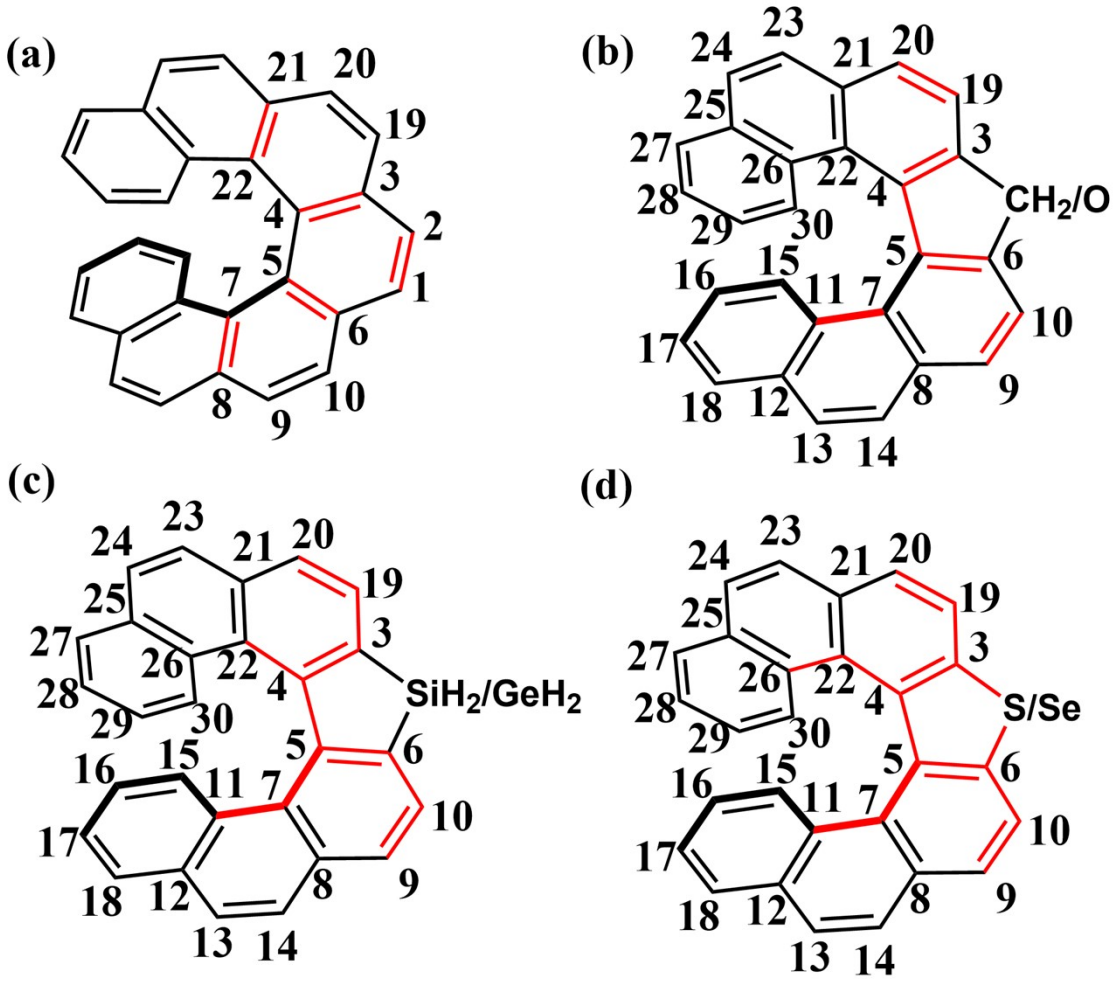

Figure S1. Considerable bond lengths variations (marked as red) between S_0 and S_1 states for [7]helicene and its derivatives.

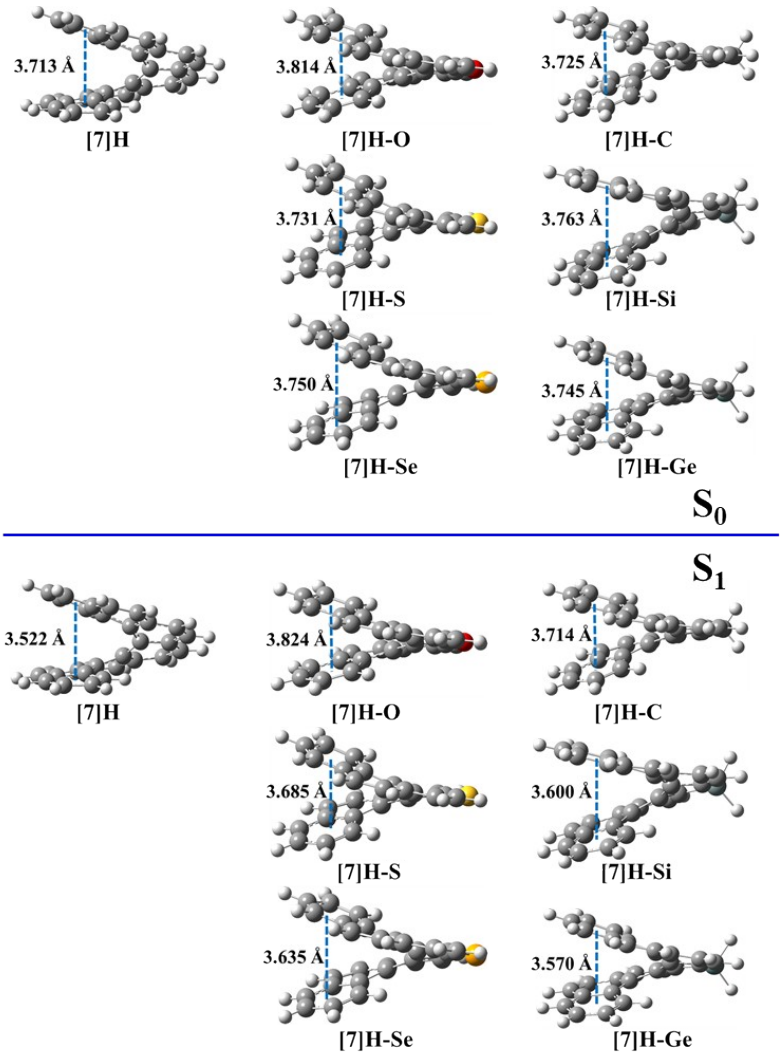

Figure S2. Centroid distances (d_c) of the two terminal benzene rings in [7]helicene and its derivatives at S_0 and S_1 states.

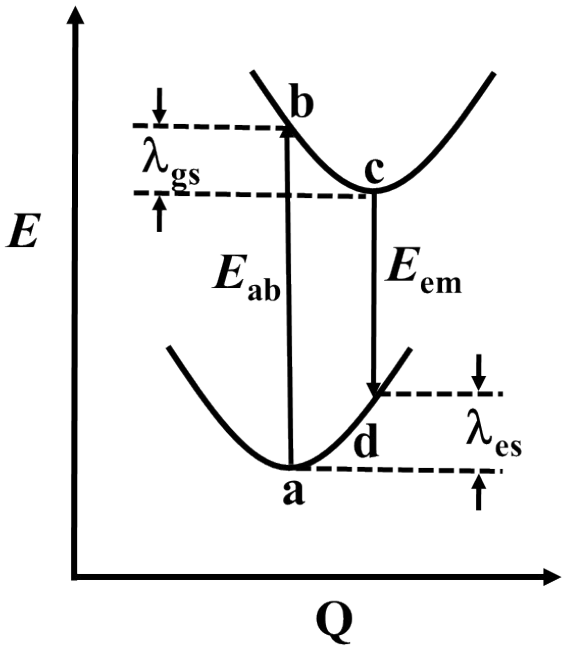

Figure S3. Schematic representation of the adiabatic potential energy surfaces for S_0 and S_1, Q is the nuclear configuration.

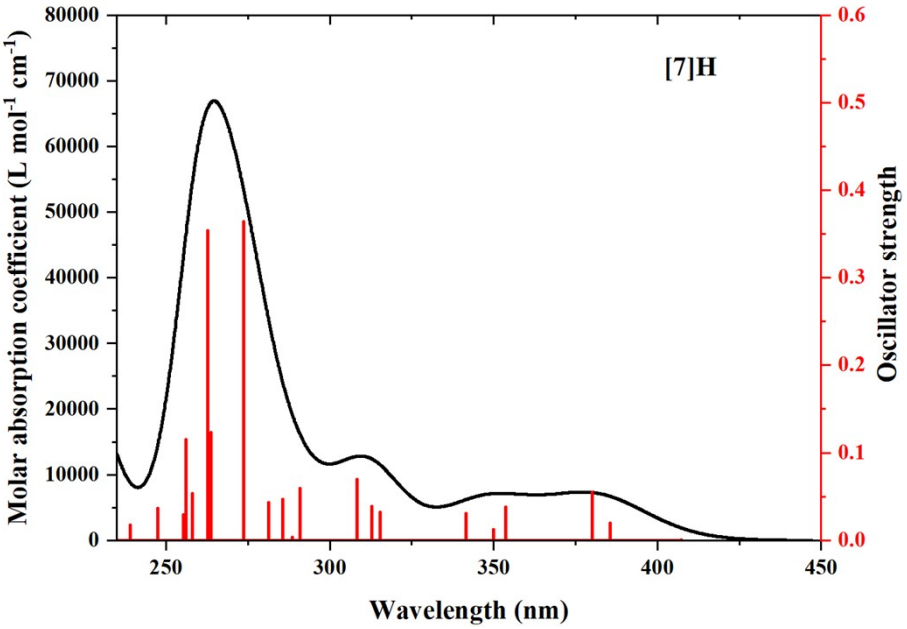
[7]H
Molar absorption coefficient (L mol-1 cm-1)
Oscillator strength
Wavelength (nm)
0
10000
20000
30000
40000
50000
60000
70000
80000
0.0
0.1
0.2
0.3
0.4
0.5
0.6
250
300
350
400
450

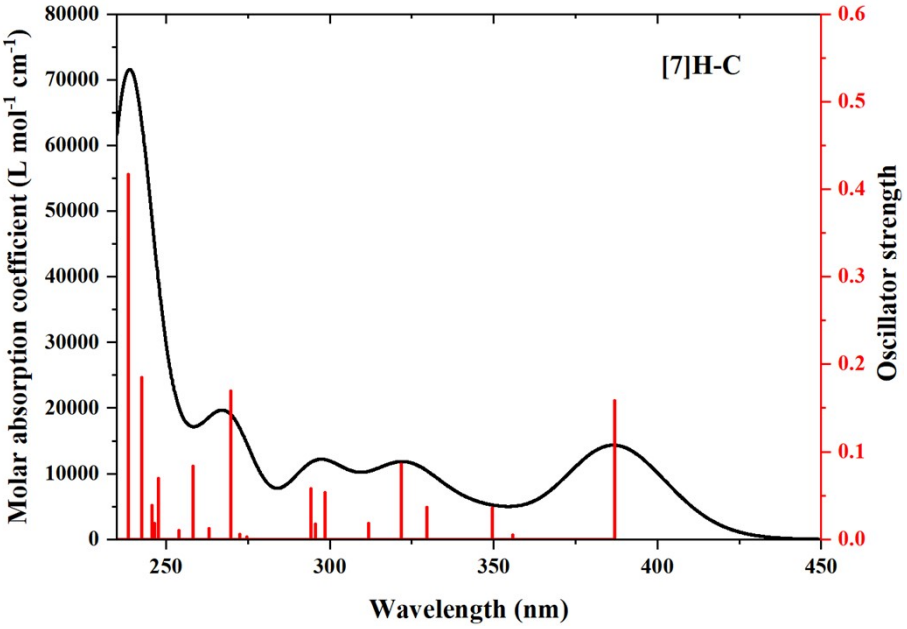
[7]H-C
Molar absorption coefficient (L mol-1 cm-1)
Oscillator strength
Wavelength (nm)
0
10000
20000
30000
40000
50000
60000
70000
80000
0.0
0.1
0.2
0.3
0.4
0.5
0.6
250
300
350
400
450

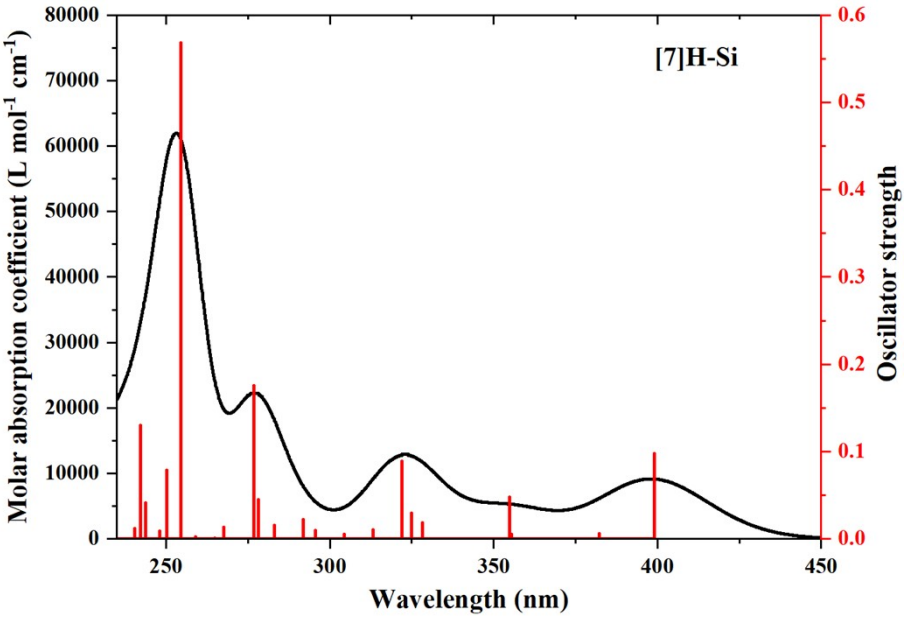
[7]H-Si
Molar absorption coefficient (L mol-1 cm-1)
Oscillator strength
Wavelength (nm)
0
10000
20000
30000
40000
50000
60000
70000
80000
0.0
0.1
0.2
0.3
0.4
0.5
0.6
250
300
350
400
450

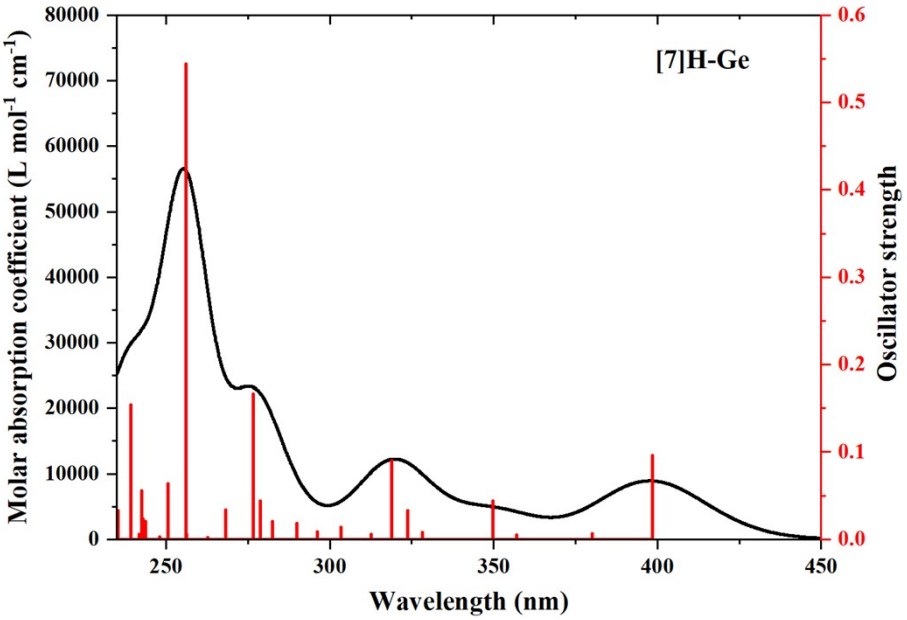
[7]H-Ge
Molar absorption coefficient (L mol-1 cm-1)
Oscillator strength
Wavelength (nm)
0
10000
20000
30000
40000
50000
60000
70000
80000
0.0
0.1
0.2
0.3
0.4
0.5
0.6
250
300
350
400
450

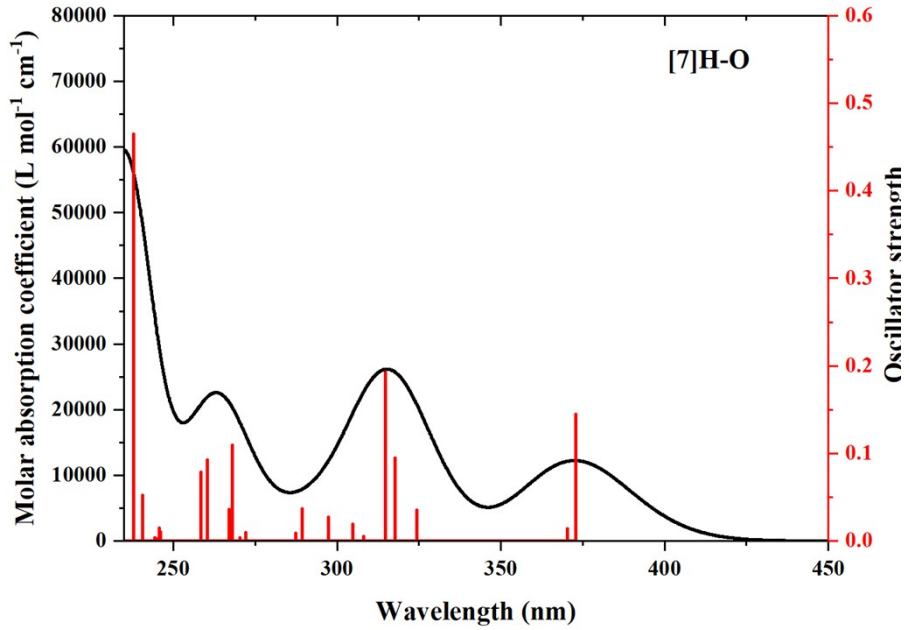
[7]H-O
Molar absorption coefficient (L mol^{-1} cm^{-1})
Oscillator strength
Wavelength (nm)
80000
70000
60000
50000
40000
30000
20000
10000
0
0.6
0.5
0.4
0.3
0.2
0.1
0.0
250
300
350
400
450

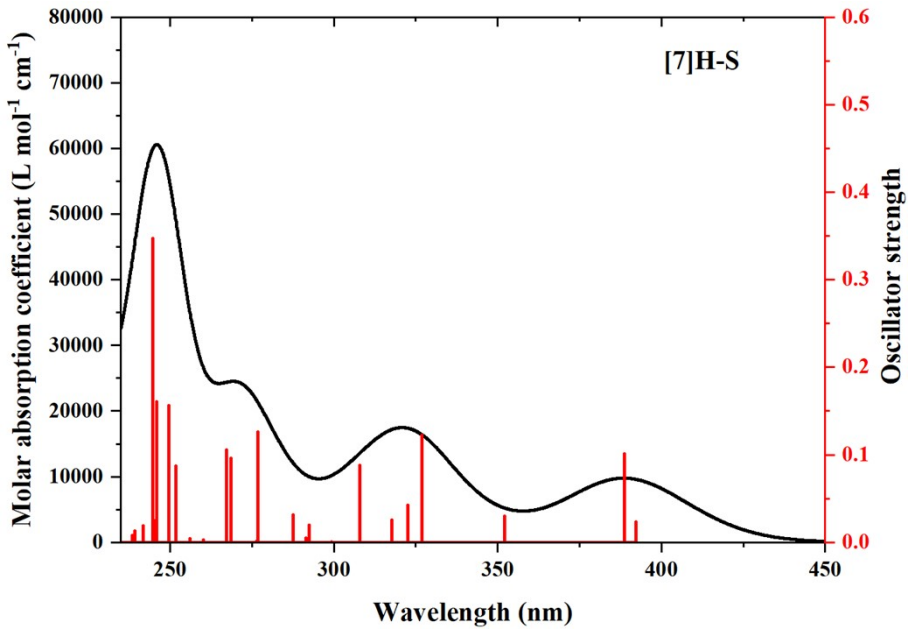
[7]H-S
Molar absorption coefficient (L mol^{-1} cm^{-1})
Oscillator strength
Wavelength (nm)
80000
70000
60000
50000
40000
30000
20000
10000
0
0.6
0.5
0.4
0.3
0.2
0.1
0.0
250
300
350
400
450

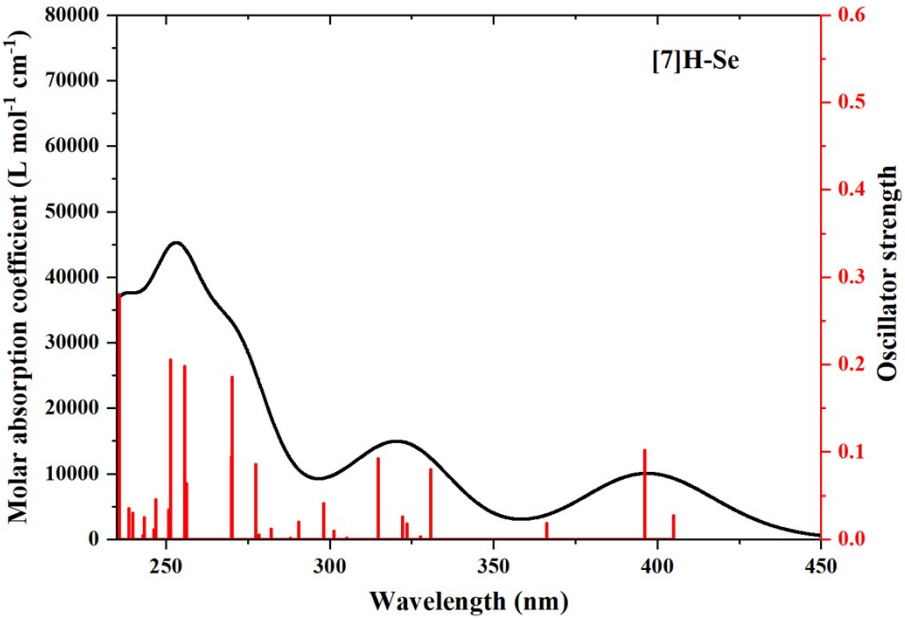

Figure S4. Calculated UV-vis spectra and oscillator strengths of the helicenes.

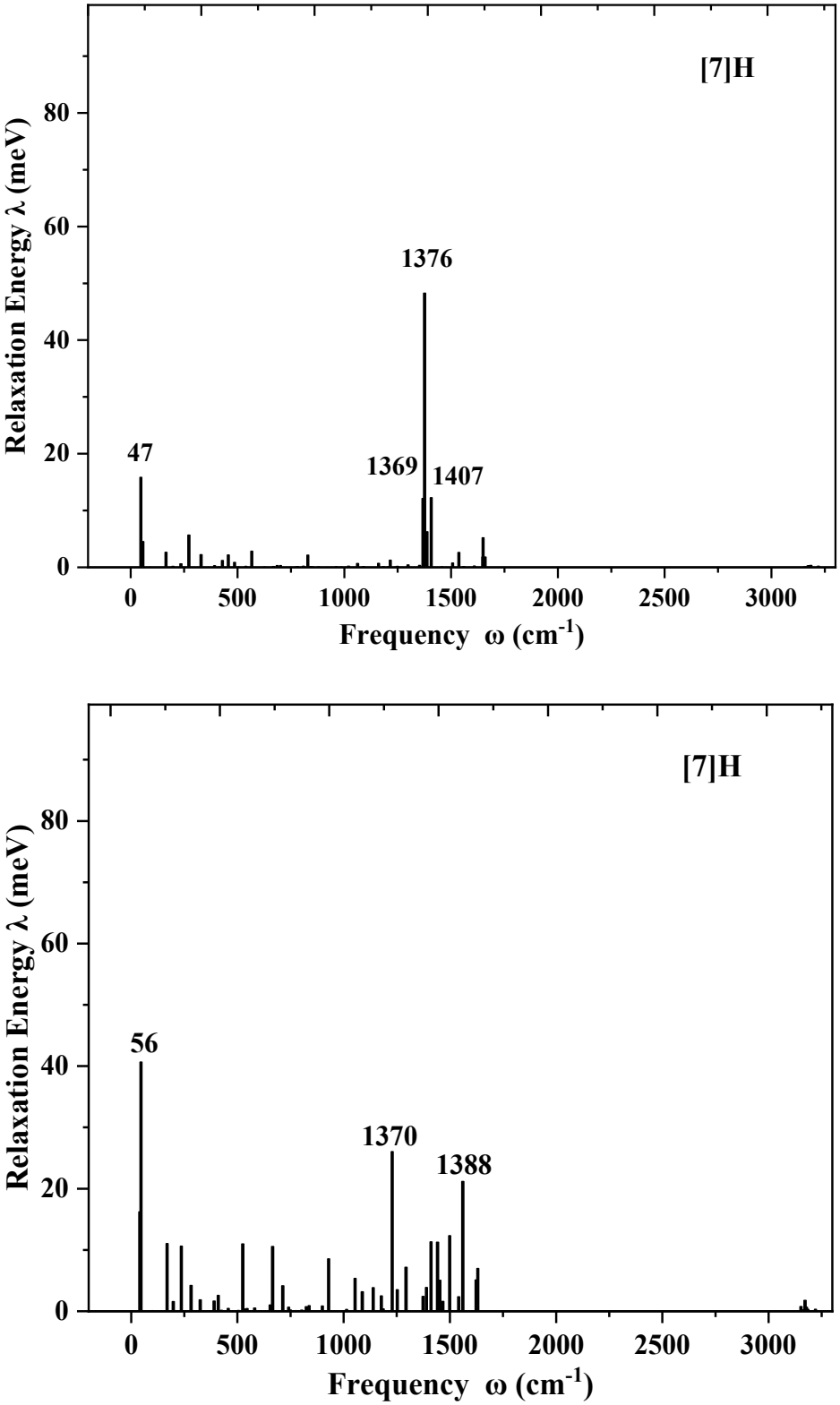

Figure S5. Calculated reorganization energy versus normal mode frequencies in solution phase of **[7]H** at S_0 (top) and S_1 (bottom) states.

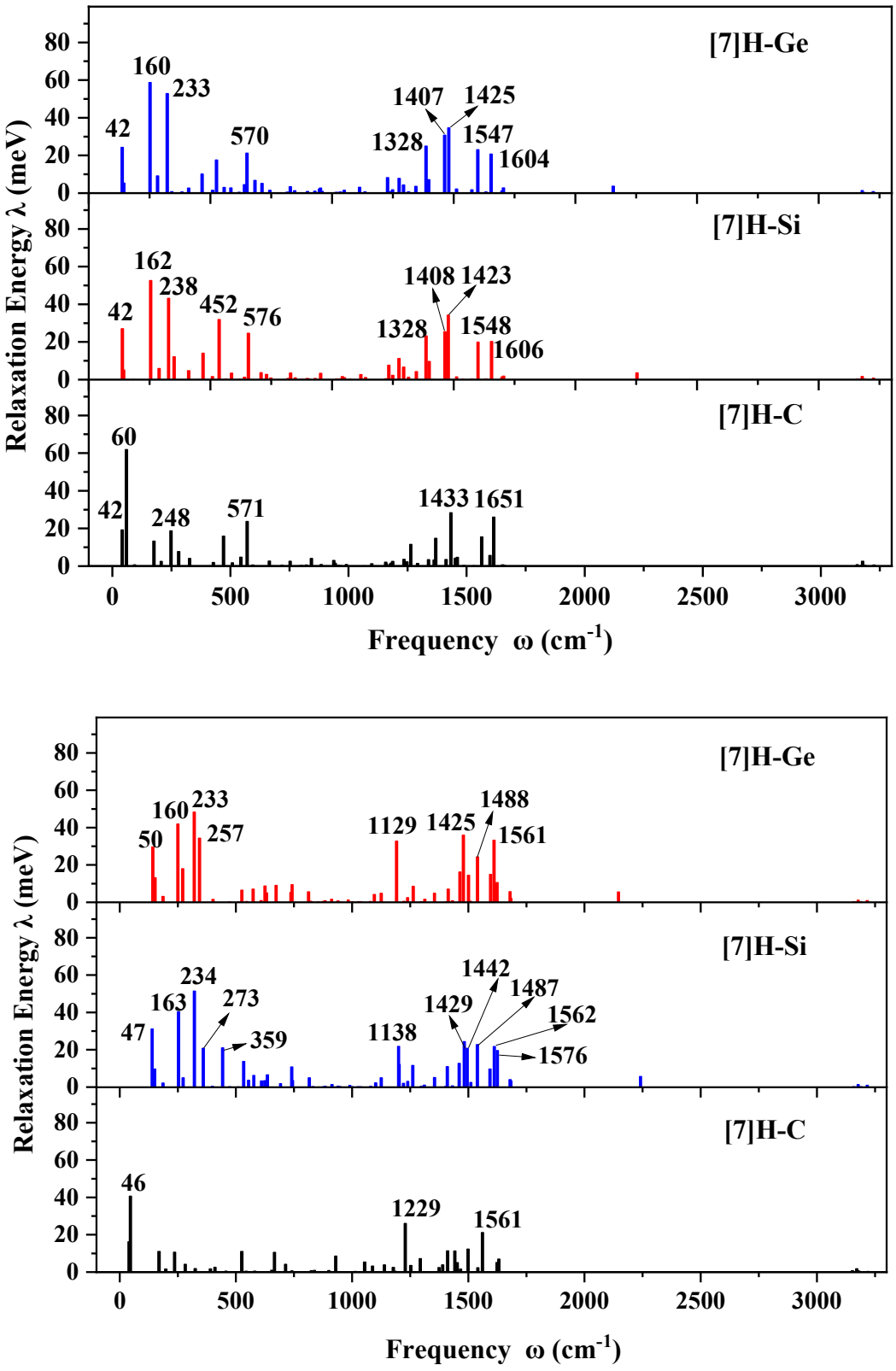

Figure S6. Calculated reorganization energy versus normal mode frequencies in solution phase of carbon group **[7]H** derivations at S_0 (top) and S_1 (bottom) states.

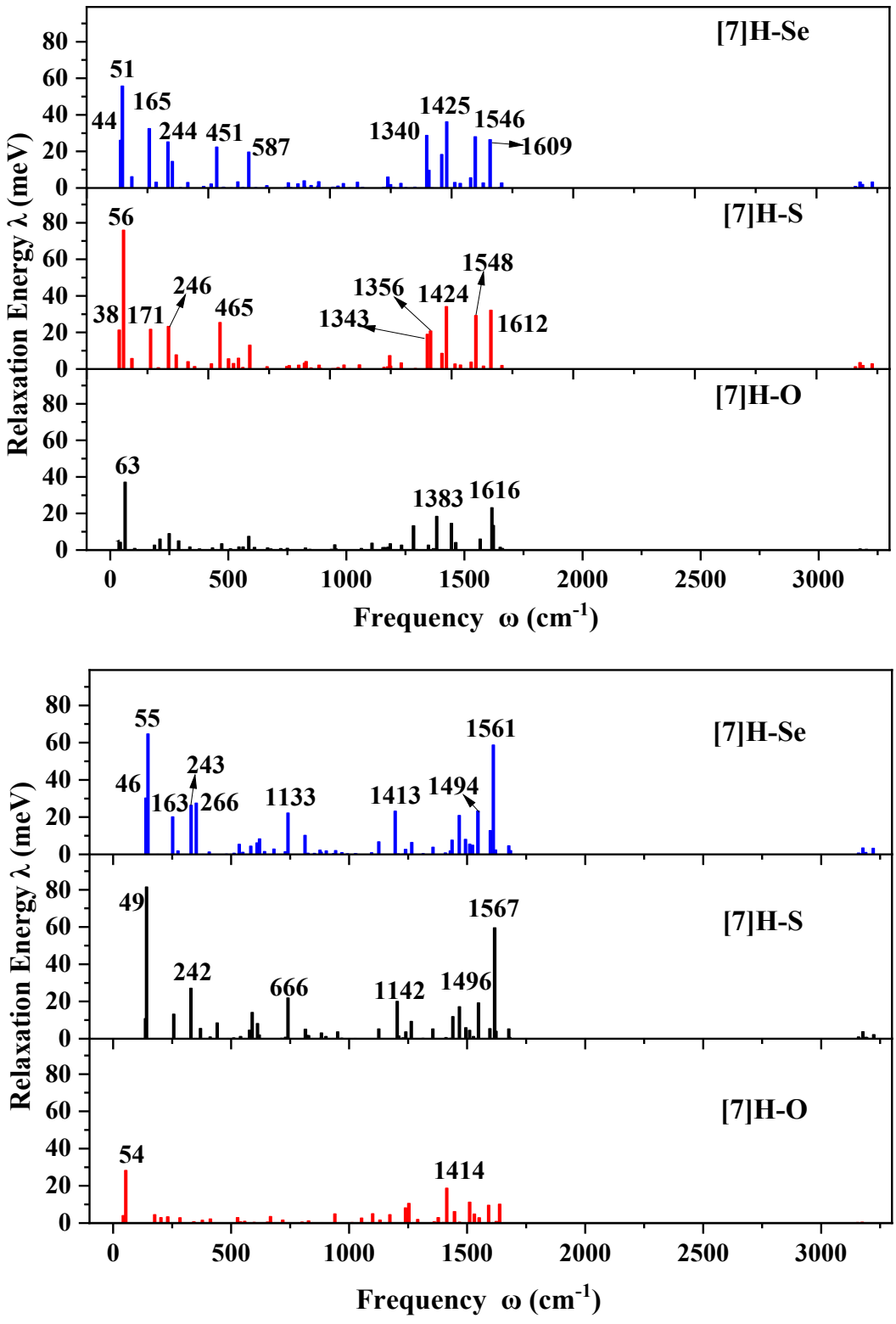

Figure S7. Calculated reorganization energy versus normal mode frequencies in solution phase of oxygen group **[7]H** derivations at S_0 (top) and S_1 (bottom) states.

[7]H (S_0)

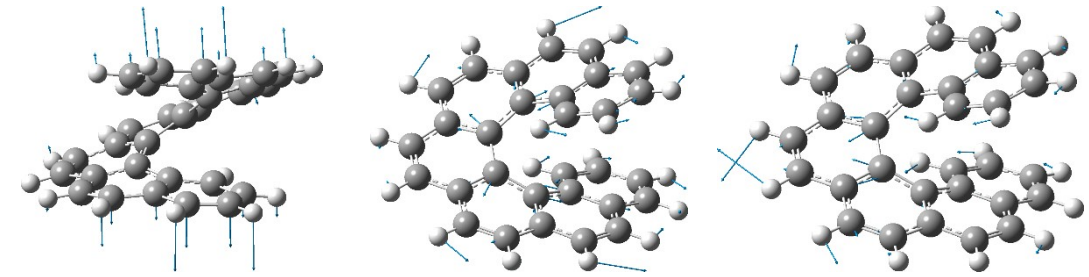

47 cm^{-1} 1369 cm^{-1} 1376 cm^{-1}

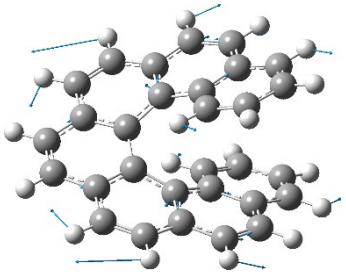

1407 cm^{-1}

[7]H (S_1)

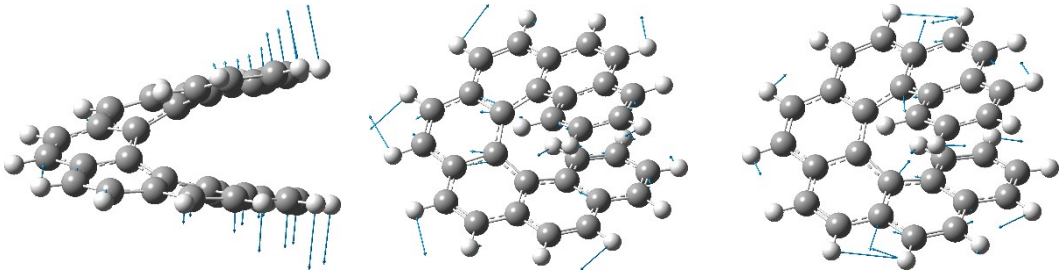

56 cm^{-1} 1370 cm^{-1} 1388 cm^{-1}

Figure S8. Selected normal modes of **[7]H** at S_0 and S_1 states with prominent relaxation energies.

[7]H-C (S_0)

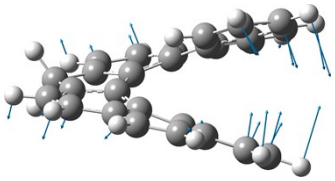

42 cm^{-1}

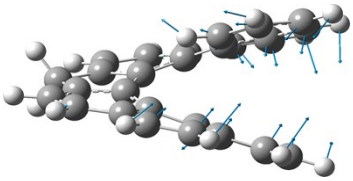

60 cm^{-1}

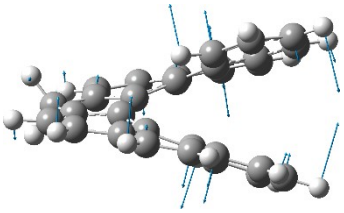

248 cm^{-1}

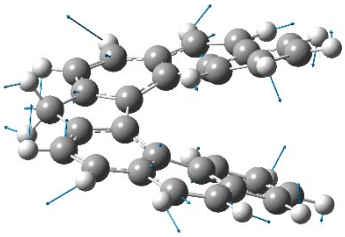

571 cm^{-1}

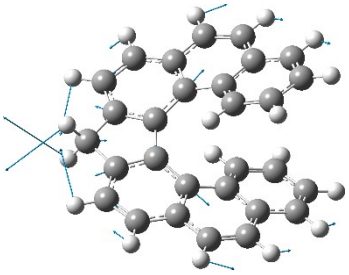

1433 cm^{-1}

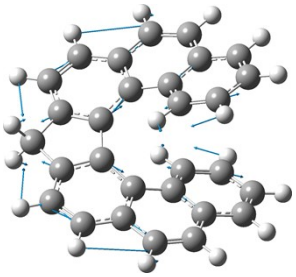

1615 cm^{-1}

[7]H-C (S_1)

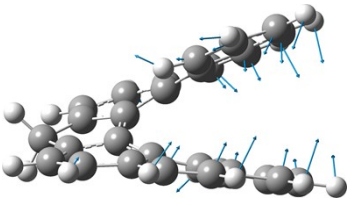

46 cm^{-1}

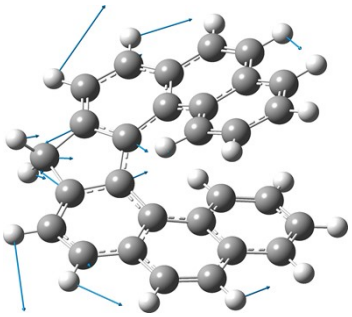

1229 cm^{-1}

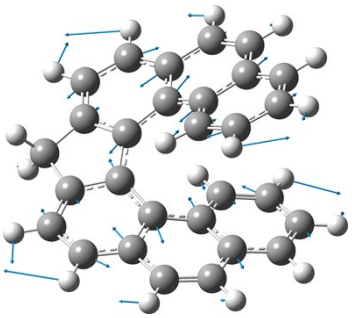

1561 cm^{-1}

[7]H-Si (S_0)

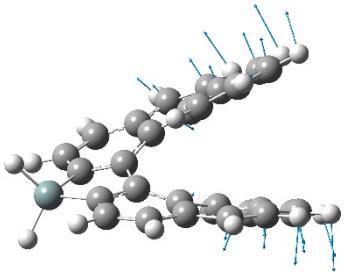

42 cm^{-1}

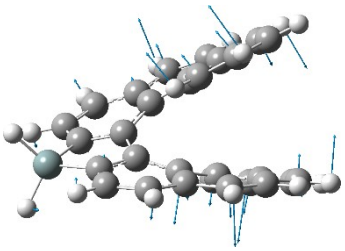

162 cm^{-1}

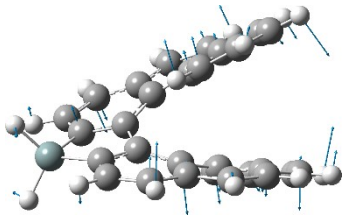

238 cm^{-1}

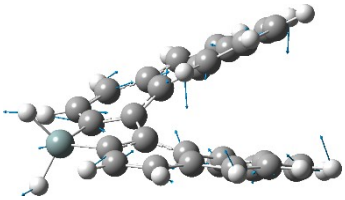

452 cm^{-1}

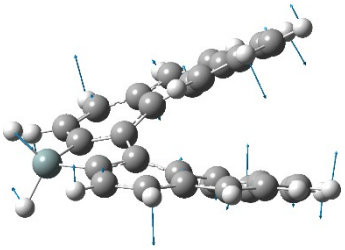

576 cm^{-1}

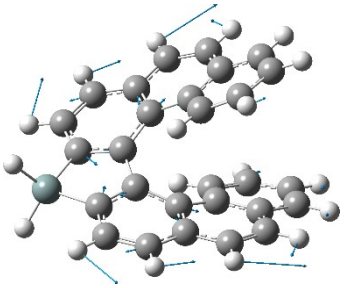

1328 cm^{-1}

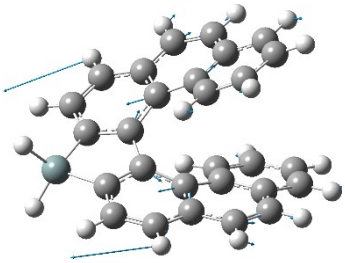

1408 cm^{-1}

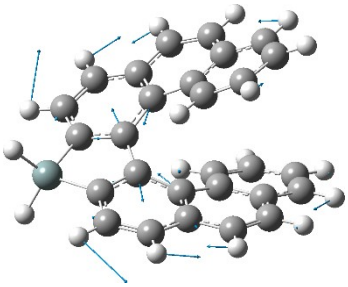

1423 cm^{-1}

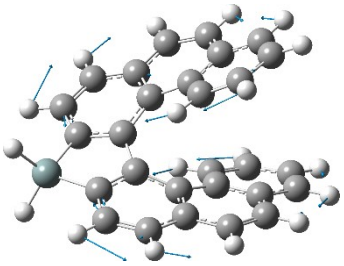

1548 cm^{-1}

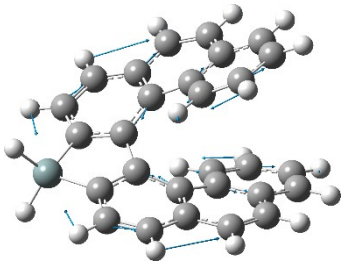

1606 cm^{-1}

[7]H-Si (S_1)

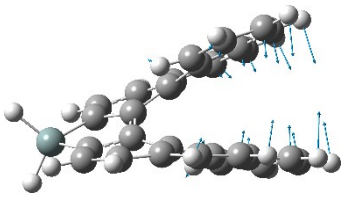

47 cm^{-1}

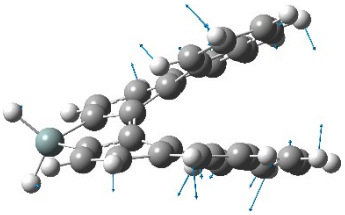

163 cm^{-1}

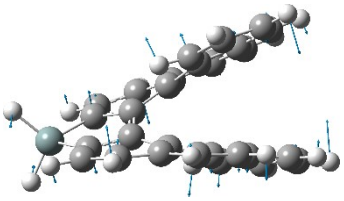

234 cm^{-1}

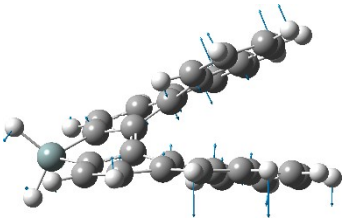

273 cm^{-1}

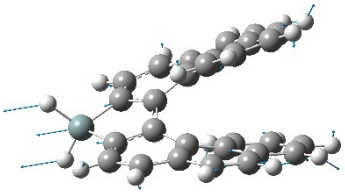

359 cm^{-1}

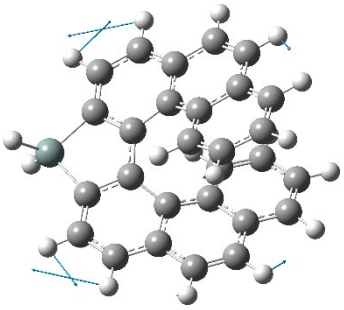

1138 cm^{-1}

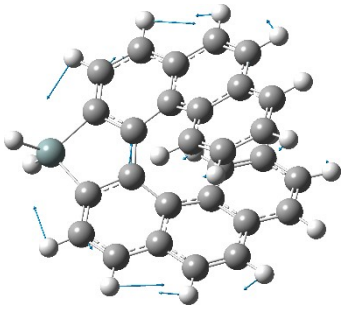

1429 cm^{-1}

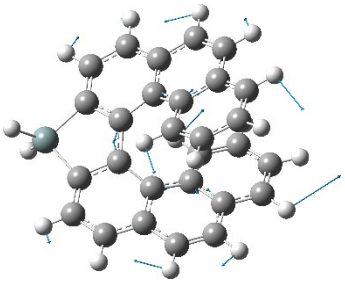

1442 cm^{-1}

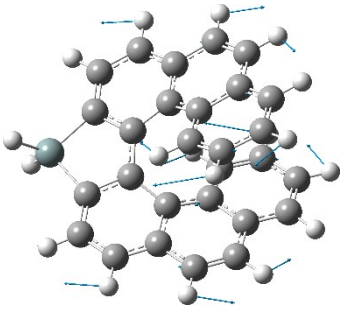

1487 cm^{-1}

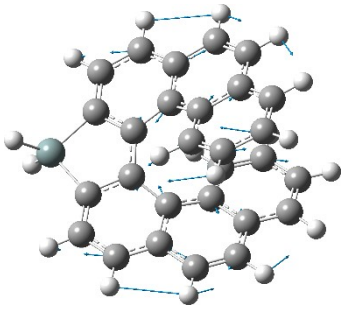

1562 cm^{-1}

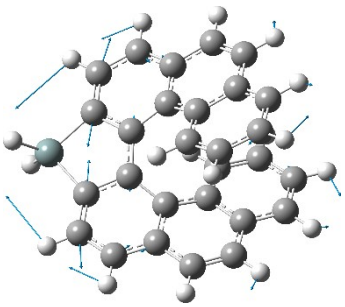

1576 cm^{-1}

[7]H-Ge (S_0)

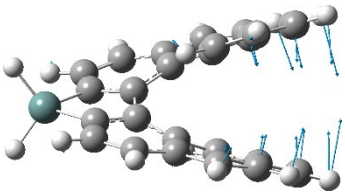

42 cm^{-1}

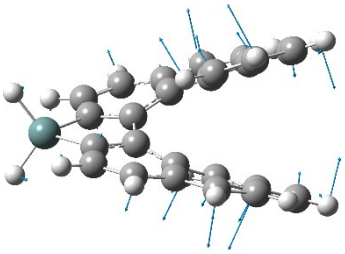

160 cm^{-1}

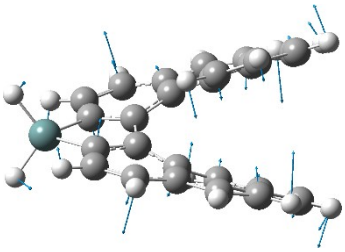

233 cm^{-1}

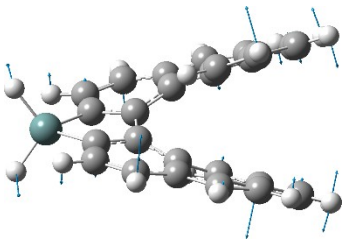

570 cm^{-1}

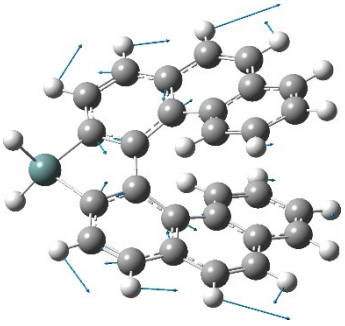

1328 cm^{-1}

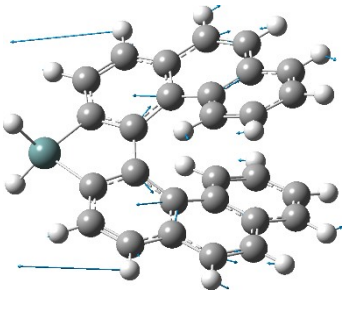

1407 cm^{-1}

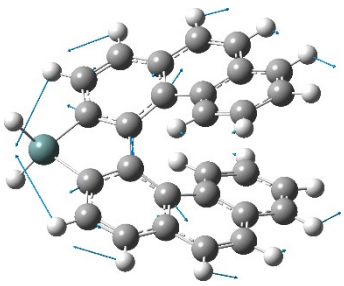

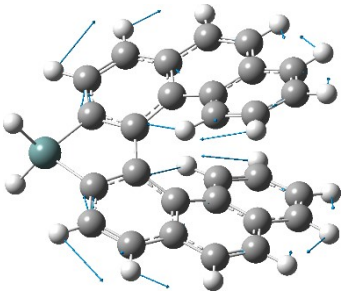

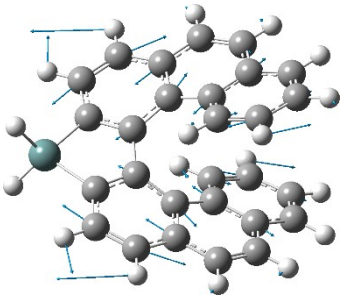

1425 cm^{-1} 1547 cm^{-1} 1604 cm^{-1}

[7]H-Ge (S_1)

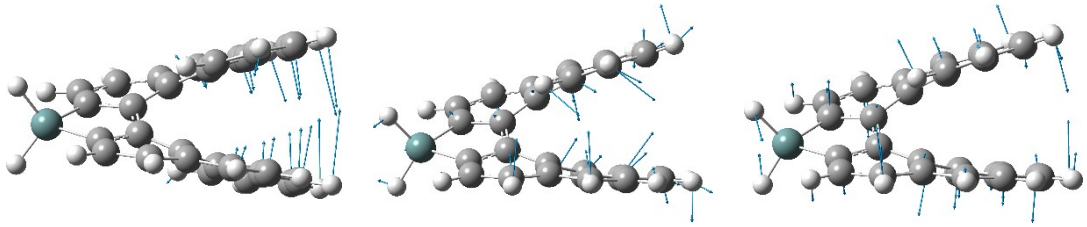

50 cm^{-1} 160 cm^{-1} 233 cm^{-1}

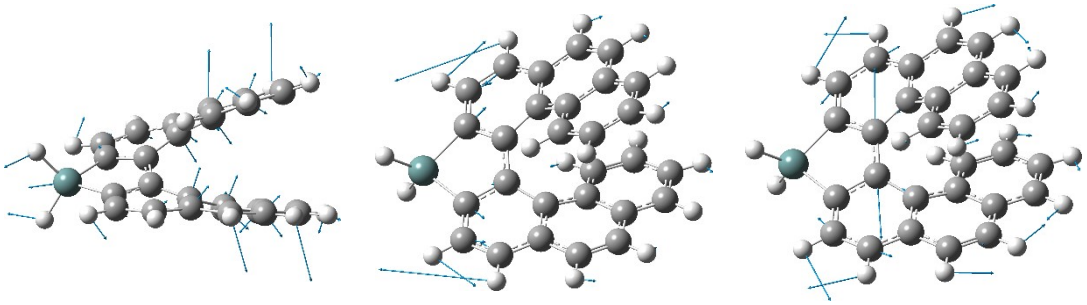

257 cm^{-1} 1129 cm^{-1} 1425 cm^{-1}

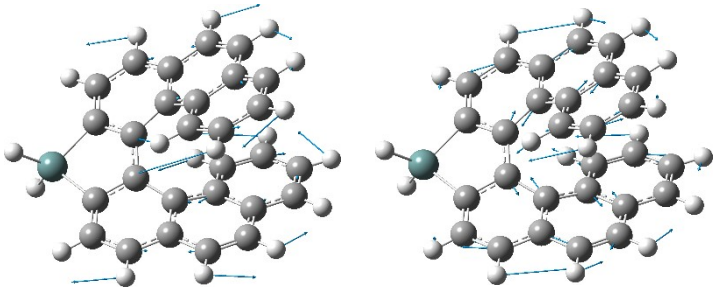

1488 cm^{-1} 1561 cm^{-1}

Figure S9. Selected normal modes of **[7]H-C**, **[7]H-Si**, and **[7]H-Ge** at both S_0 and S_1 states with prominent relaxation energies.

[7]H-O (S_0)

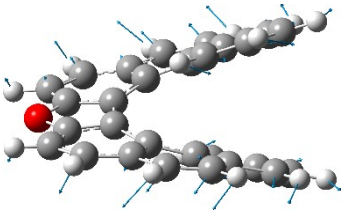

63 cm^{-1}

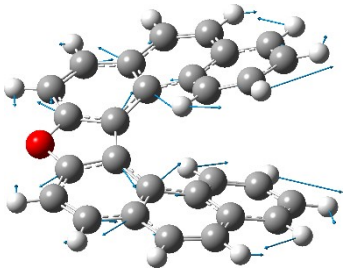

1383 cm^{-1}

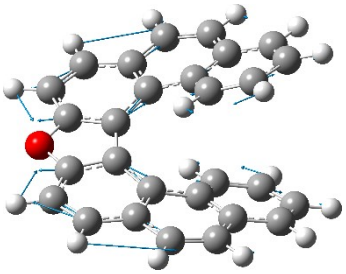

1616 cm^{-1}

[7]H-O (S_1)

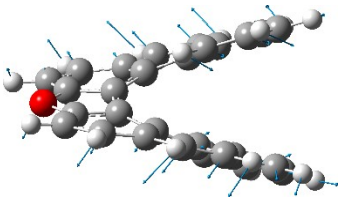

54 cm^{-1}

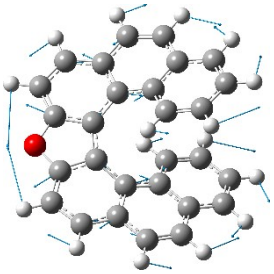

1414 cm^{-1}

[7]H-S (S_0)

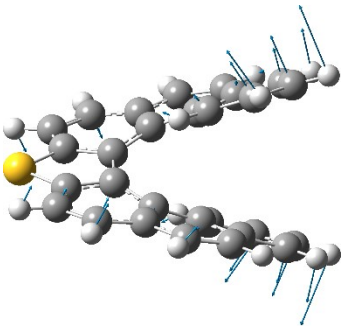

38 cm^{-1}

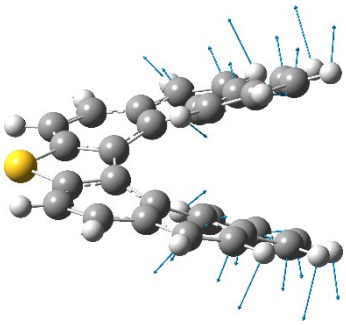

56 cm^{-1}

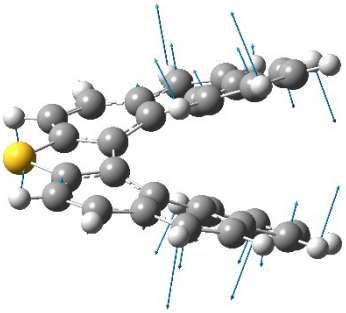

171 cm^{-1}

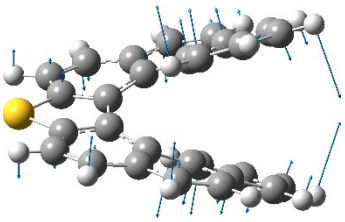

246 cm^{-1}

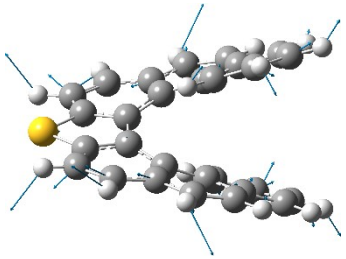

465 cm^{-1}

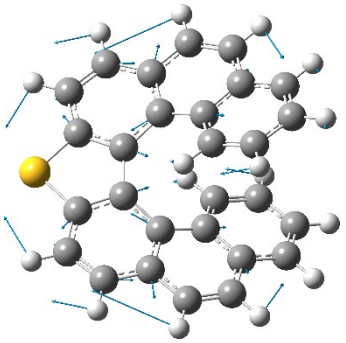

1343 cm^{-1}

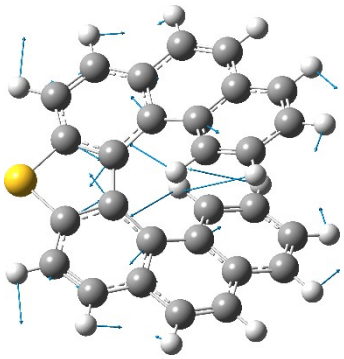

1356 cm^{-1}

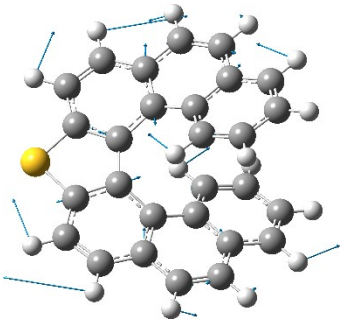

1424 cm^{-1}

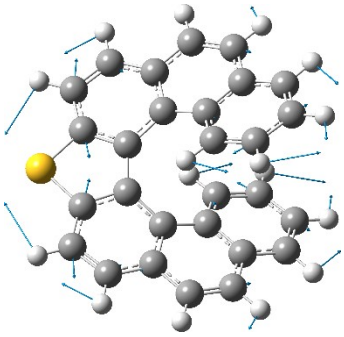

1548 cm^{-1}

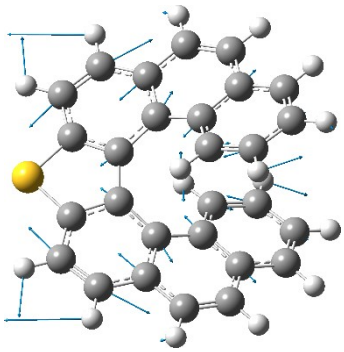

1612 cm^{-1}

[7]H-S (S_1)

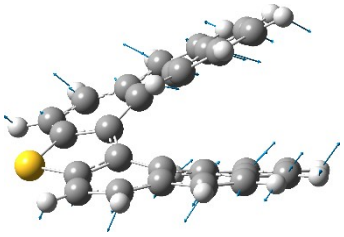

49 cm^{-1}

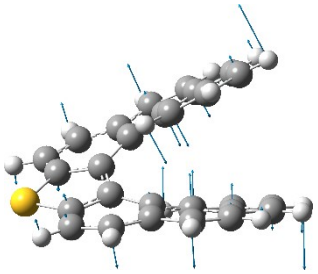

242 cm^{-1}

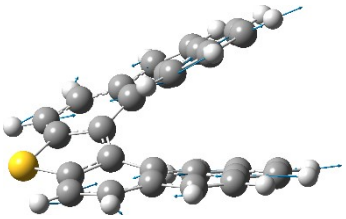

666 cm^{-1}

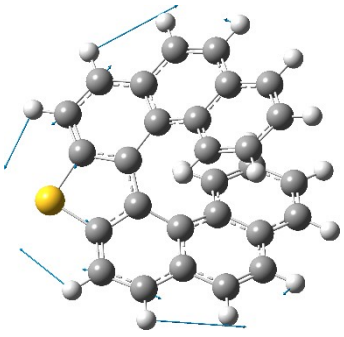

1142 cm^{-1}

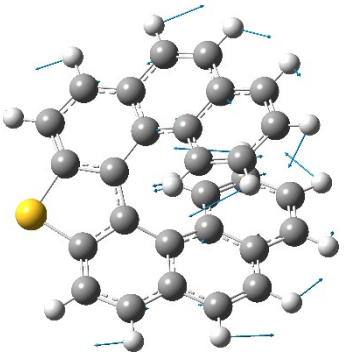

1496 cm^{-1}

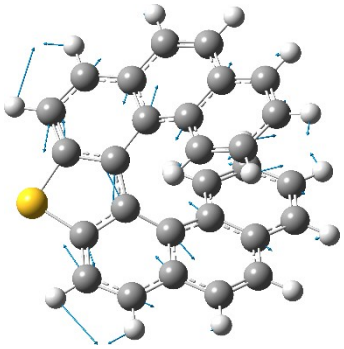

1567 cm^{-1}

[7]H-Se (S_0)

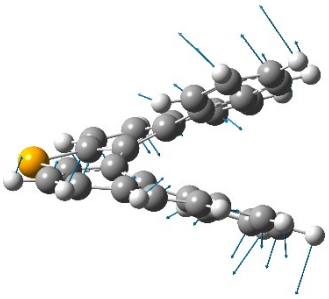

44 cm^{-1}

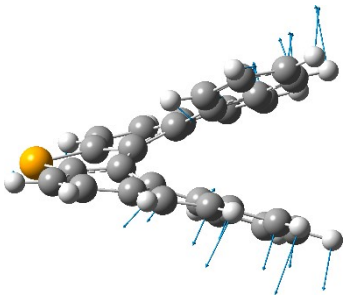

51 cm^{-1}

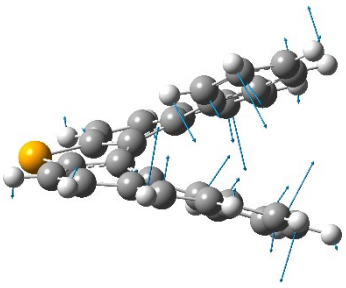

165 cm^{-1}

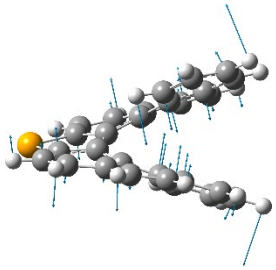

244 cm^{-1}

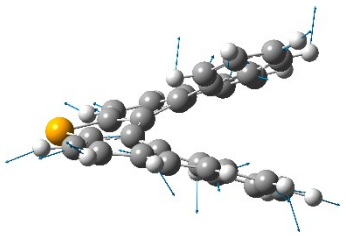

451 cm^{-1}

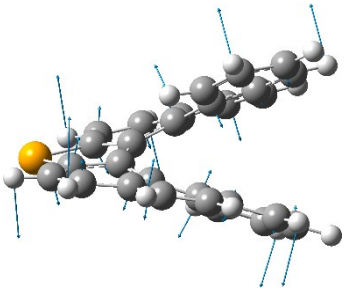

587 cm^{-1}

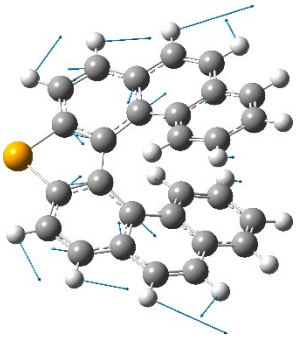

1340 cm^{-1}

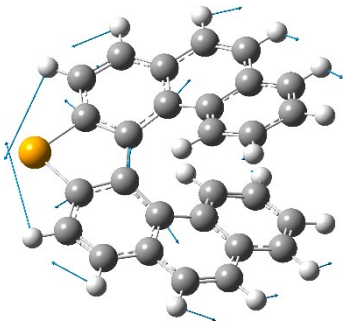

1425 cm^{-1}

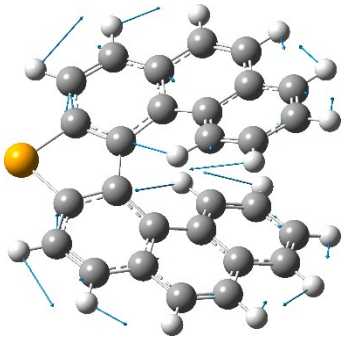

1546 cm^{-1}

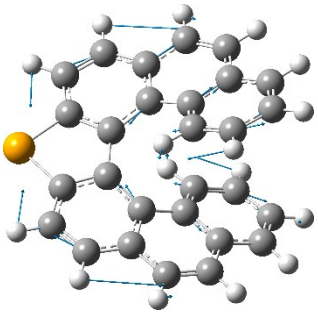

1609 cm^{-1}

[7]H-Se (S_1)

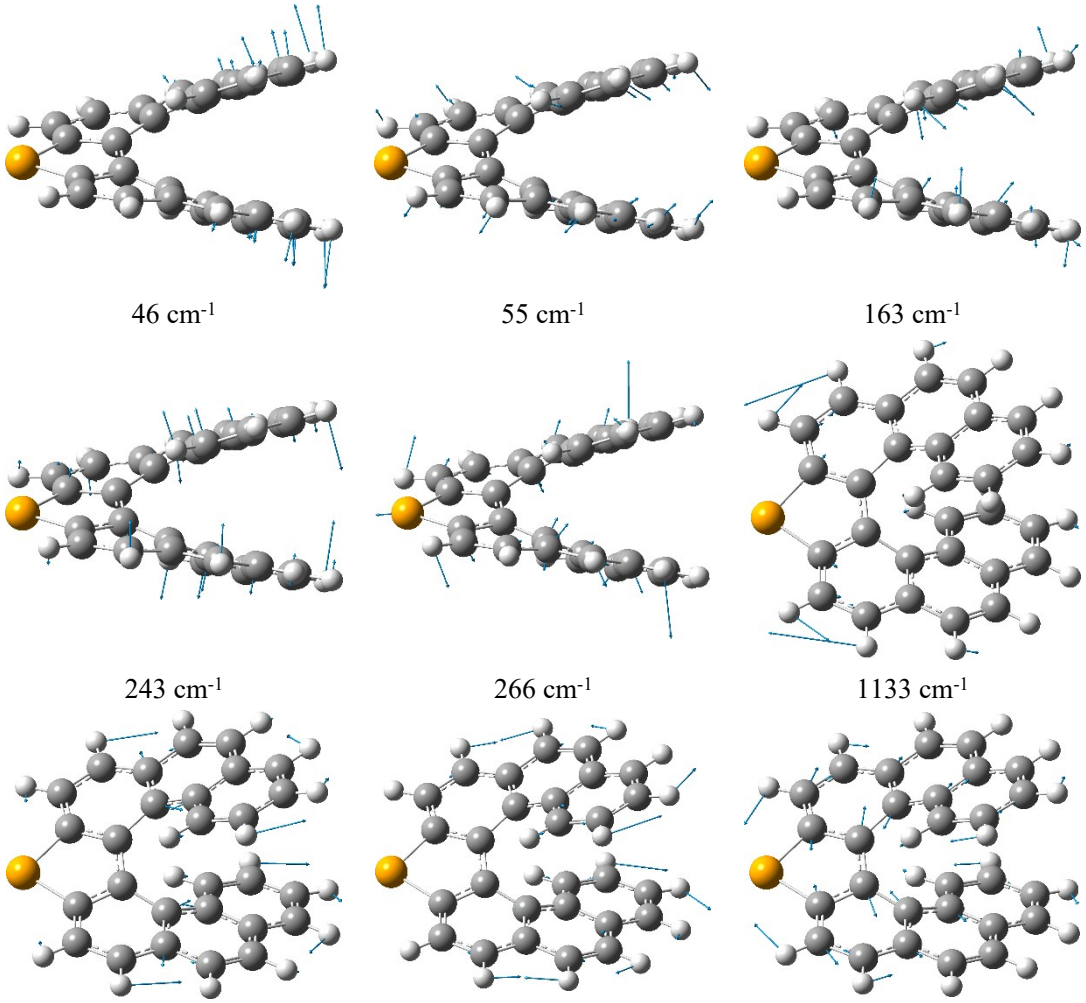

Figure S10. Selected normal modes of **[7]H-O**, **[7]H-S**, and **[7]H-Se** at both S_0 and S_1 states with prominent relaxation energies.

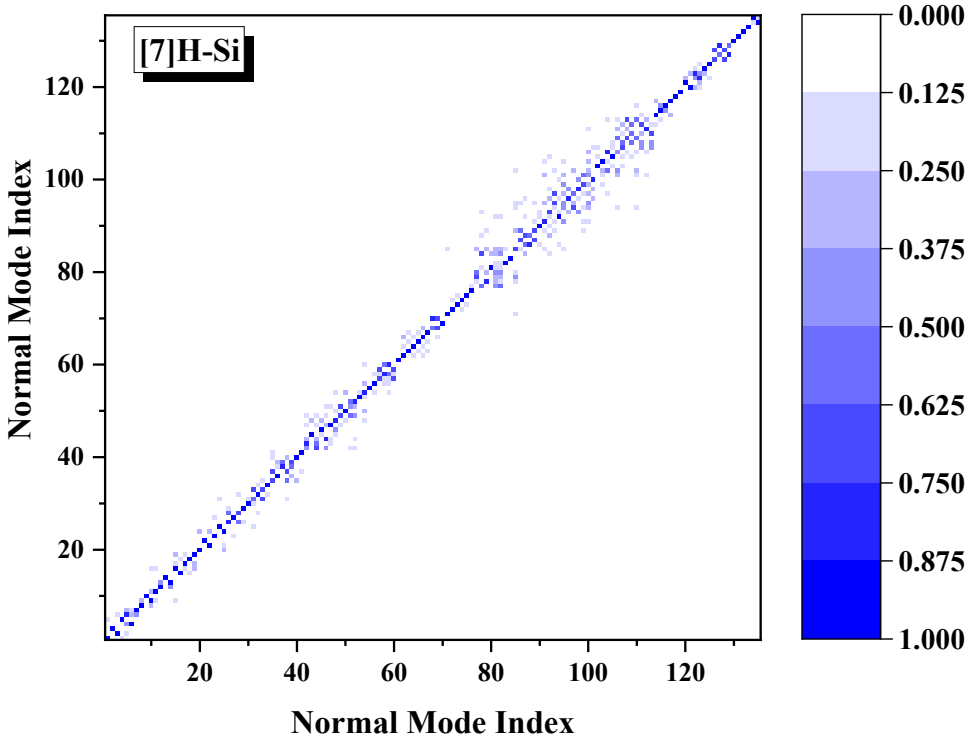
[7]H-Si
Normal Mode Index
Normal Mode Index
20
40
60
80
100
120
0.000
0.125
0.250
0.375
0.500
0.625
0.750
0.875
1.000

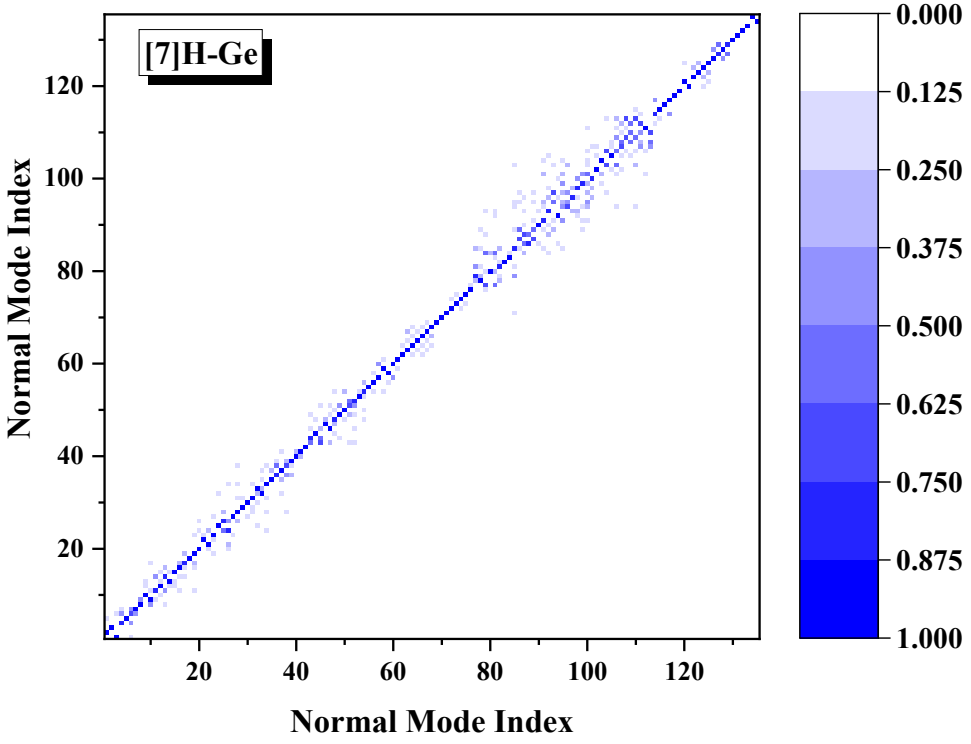
[7]H-Ge
Normal Mode Index
Normal Mode Index
20
40
60
80
100
120
0.000
0.125
0.250
0.375
0.500
0.625
0.750
0.875
1.000

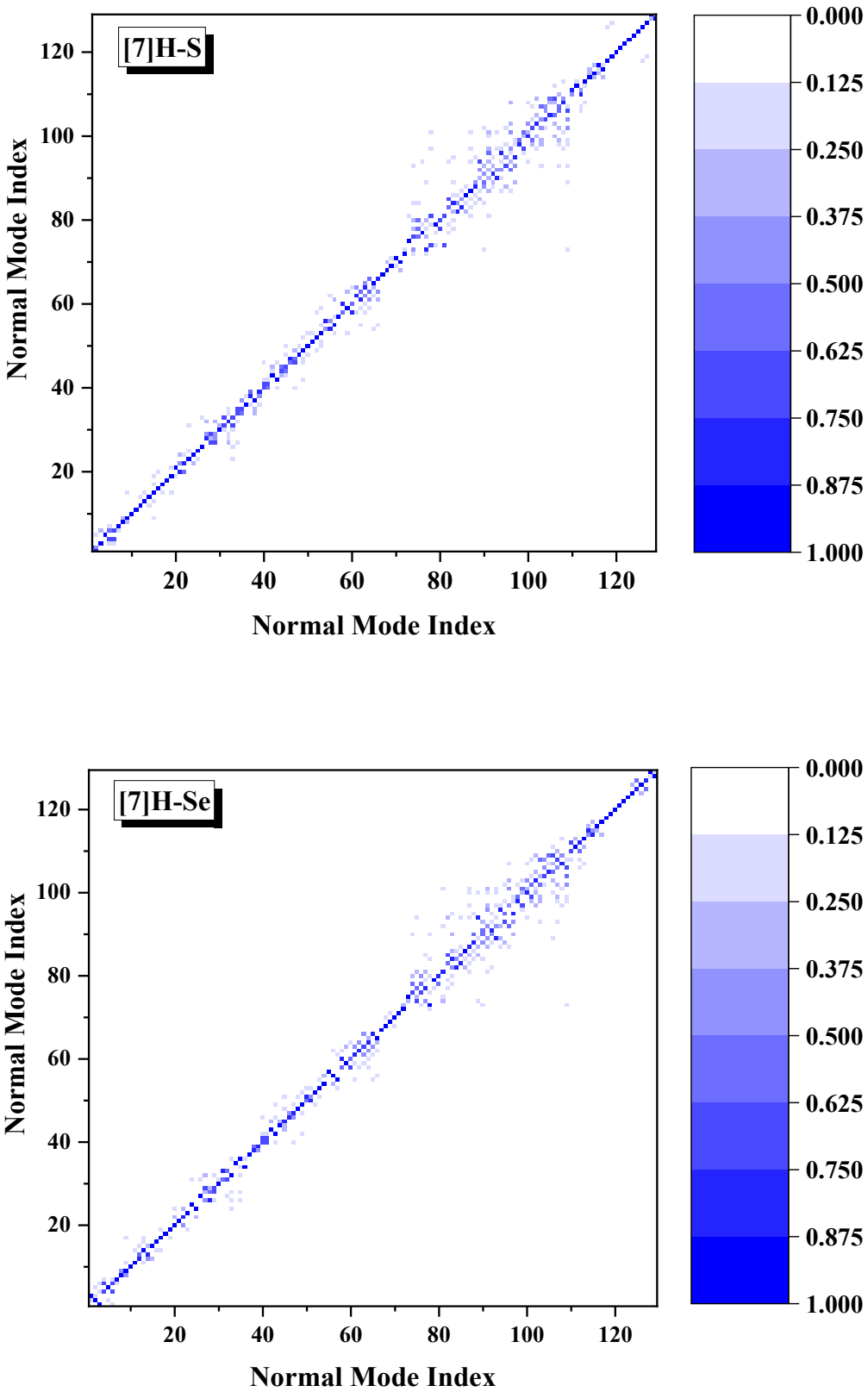

Figure S11. Contour maps of the Dushinsky rotation matrix of **[7]H-Si**, **[7]H-Ge**, **[7]H-S**, and **[7]H-Se**.

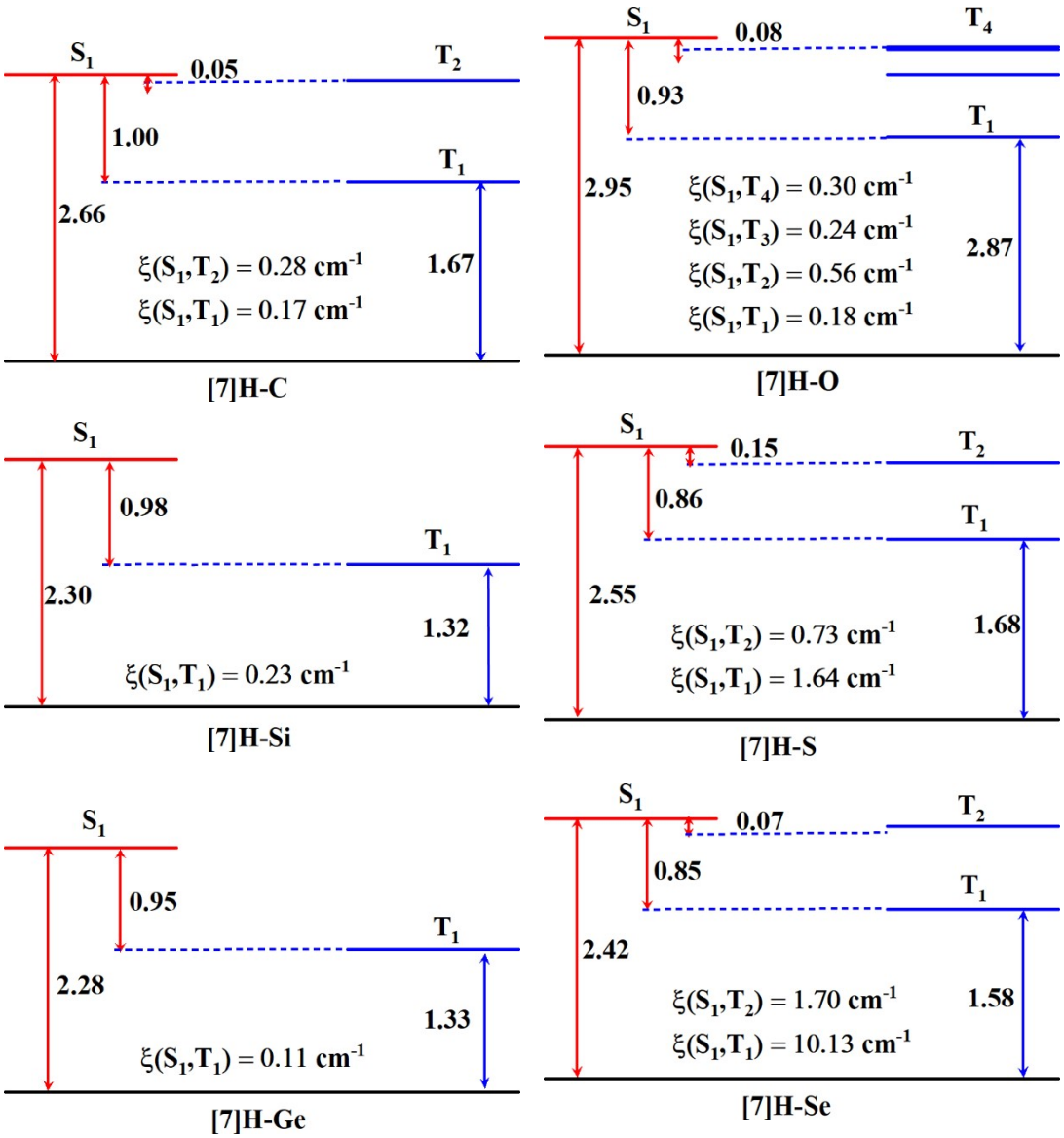

Figure 12. Energy level diagrams and SOC coefficients (ξ).

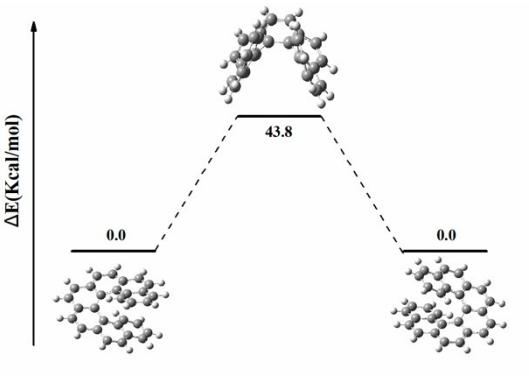

[7]H

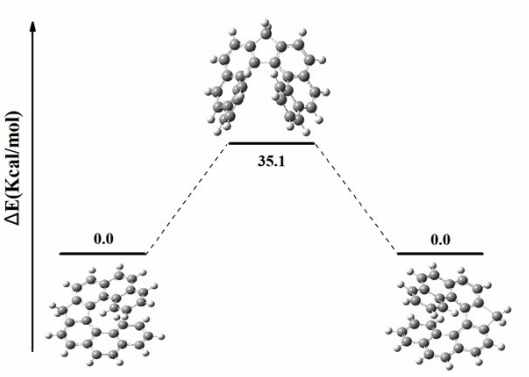

[7]H-C

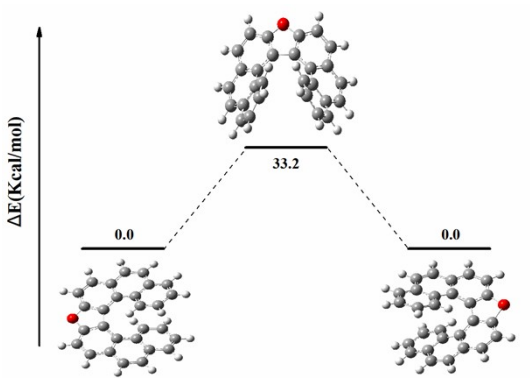

[7]H-O

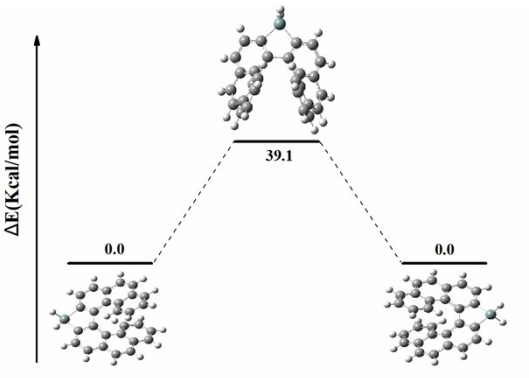

[7]H-Si

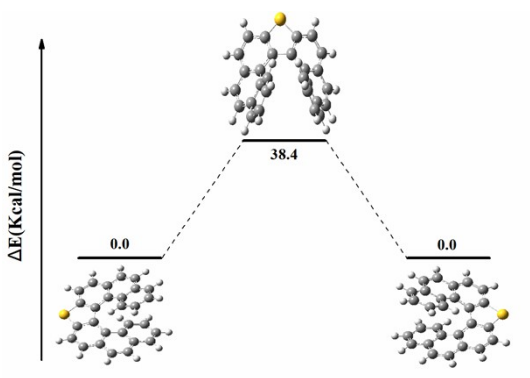

[7]H-S

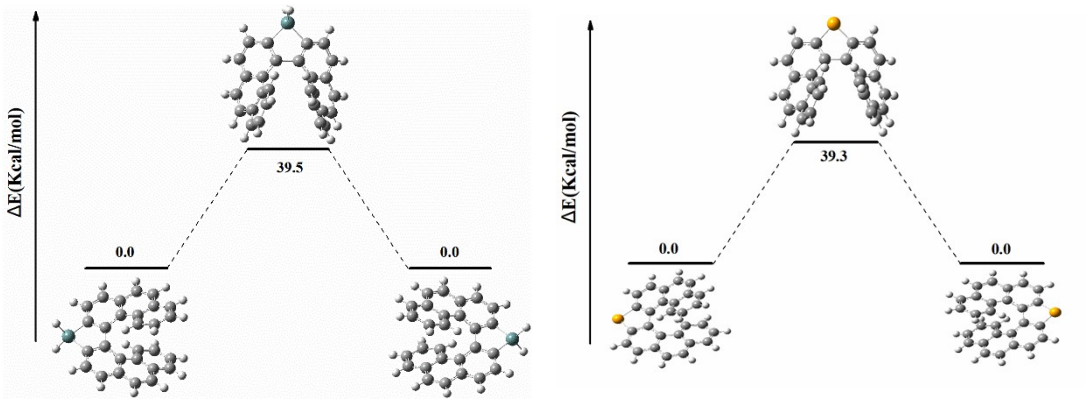

[7]H-Ge **[7]H-Se**

Figure S13. Energy profiles and transition states of [7]helicene and its derivatives. The barriers are in kcal/mol.